Advances in Colloid and Interface Science 321 (2023) 103007

Contents lists available at ScienceDirect

Advances in Colloid and Interface Science

journal homepage: www.elsevier.com/locate/cis

Historical Perspective

Core–shell inorganic NP@MOF nanostructures for targeted drug delivery and multimodal imaging-guided combination tumor treatment

Suliman Khan [a], Mojtaba Falahati [b,c,*], William C. Cho [d], Yasaman Vahdani [e], Rabeea Siddique [a], Majid Sharifi [f,g], Laila Abdulmohsen Jaragh-Alhadad [h], Setareh Haghighat [i], Xiaoju Zhang [j], Timo L.M. ten Hagen [b,c,*], Qian Bai [a,**]

[a] Medical Research Center, The Second Affiliated Hospital of Zhengzhou University, Zhengzhou, China
[b] Precision Medicine in Oncology (PrMiO), Department of Pathology, Erasmus MC Cancer Institute, Erasmus MC, Rotterdam, the Netherlands
[c] Nanomedicine Innovation Center Erasmus (NICE), Erasmus MC, Rotterdam, the Netherlands
[d] Department of Clinical Oncology, Queen Elizabeth Hospital, Kowloon, Hong Kong SAR, China
[e] Department of Biochemistry and Molecular Medicine, University of Montreal, Canada
[f] Student Research Committee, School of Medicine, Shahroud University of Medical Sciences, Shahroud, Iran
[g] Department of Tissue Engineering, School of Medicine, Shahroud University of Medical Sciences, Shahroud, Iran
[h] Department of Chemistry, College of Science, Kuwait University, Safat 13060, Kuwait
[i] Department of Microbiology, Faculty of Advanced Sciences and Technology, Tehran Medical Sciences, Islamic Azad University, Tehran, Iran
[j] Department of Respiratory and Critical Care Medicine, Henan Provincial People's Hospital, Zhengzhou, China

ARTICLE INFO

Keywords:
Core–shell metal–organic framework
Imaging
Cancer therapy
Drug delivery

ABSTRACT

It is well known that metal–organic framework (MOF) nanostructures have unique characteristics such as high porosity, large surface areas and adjustable functionalities, so they are ideal candidates for developing drug delivery systems (DDSs) as well as theranostic platforms in cancer treatment. Despite the large number of MOF nanostructures that have been discovered, conventional MOF-derived nanosystems only have a single bio-functional MOF source with poor colloidal stability. Accordingly, developing core–shell MOF nanostructures with good colloidal stability is a useful method for generating efficient drug delivery, multimodal imaging and synergistic therapeutic systems. The preparation of core–shell MOF nanostructures has been done with a variety of materials, but inorganic nanoparticles (NPs) are highly effective for drug delivery and imaging-guided tumor treatment. Herein, we aimed to overview the synthesis of core–shell inorganic NP@MOF nanostructures followed by the application of core–shell MOFs derived from magnetic, quantum dots (QDs), gold (Au), and gadolinium (Gd) NPs in drug delivery and imaging-guided tumor treatment. Afterward, we surveyed different factors affecting prolonged drug delivery and cancer therapy, cellular uptake, biocompatibility, biodegradability, and enhanced permeation and retention (EPR) effect of core–shell MOFs. Last but not least, we discussed the challenges and the prospects of the field. We envision this article may hold great promise in providing valuable insights regarding the application of hybrid nanostructures as promising and potential candidates for multimodal imaging-guided combination cancer therapy.

1. Introduction

Given the dramatic changes in human lifestyle, cancer and its widespread prevalence have become major medical and health challenges. Cells deviate from their normal growth process and become cancerous *via* a variety of pathways, and identifying and inhibiting these processes are important functional aspects of cancer treatment. Chemotherapy has raised concerns in cancer treatment due to unwanted side effects and tumorigenic cancer cell-intrinsic resistance [1]. As a result, the ability to precisely target cancer cells *via* intelligent nano-platforms can reduce the side effects of chemotherapeutic agents while dramatically increasing patient survival.

* Corresponding authors at: Precision Medicine in Oncology (PrMiO), Department of Pathology, Erasmus MC Cancer Institute, Erasmus MC, Rotterdam, the Netherlands.
** Corresponding author.
E-mail addresses: m.falahati@erasmusmc.nl (M. Falahati), t.l.m.tenhagen@erasmusmc.nl (T.L.M. ten Hagen), baiqian@zzu.edu.cn (Q. Bai).

https://doi.org/10.1016/j.cis.2023.103007
Received in revised form 16 August 2023;
Available online 25 September 2023

Nanoparticles (NPs) as potential carriers offer a new form of drug delivery to cancer cells by delivering high concentrations of the drug specifically to the target tumor cells while minimizing the deleterious effects on noncancerous cells [2]. The advantages of using intelligent-based drug delivery *via* NPs include increased drug accumulation in target cells, improved therapeutic effects and lower toxicity [3,4]. Liposomes, micelles and other polymer-based platforms are generally used as potential nanocarriers in drug delivery and the drug release kinetics can be regulated through manipulation of composition, size and functional groups [5,6]. Also, their building blocks could be biodegradable and non-toxic substances found in all biological membranes of living organisms. However, limited stability, complex drug release kinetics and inefficient real-time tracing have introduced some challenges toward the clinical implementations of these carriers.

Inorganic nano-platforms such as silica (SiO_2) [7], Au [8], iron oxide (IO) [9,10], silver (Ag) [11], zinc oxide (ZnO) [12], and QDs [13] have shown significantly enhanced loading capacity as well as targeted drug release. However, surface functionalization processes, biocompatibility, aggregation, degradation, and internalization by tumor cells are important factors to manipulate when developing inorganic drug nanocarriers for theranostics and drug delivery applications [14,15]. Metal–organic frameworks (MOFs) with a highly regular porous crystalline structure introduced by Hoskins and Robson [16] have received a great deal of interest in the development of drug carriers for cancer therapy [17,18]. Indeed, following the application of MOFs in drug delivery [19] and a study by Babarao and Jiang [20] indicating that the maximum loading of ibuprofen in MOFs is four times greater than that in mesoporous SiO_2 NPs, their promising biological applications have been offered in different biomedical areas such as imaging, biosensing, drug delivery, and therapeutics due to their inherent high porosity and mesoporous framework [21,22]. For example, MOF NPs exhibiting hollow microspheres with high loading capacity [23,24] and encapsulated 3-methyladenine (3-MA) as an autophagy inhibitor can be used in the development of a potentially controllable DDSs against cancer therapy mediated by downregulation of autophagy-associated markers, Beclin 1 and LC3 [25].

Due to the need for multifunctional systems to mediate intelligently targeted therapy, nevertheless, sole MOFs have shown a significant shortfall in therapeutic applications. In other words, MOFs typically exhibit high electronic conductivity and drug-loading capability in nanomedicine-based cancer therapy, but their specific targeting, theranostic and anti-tumor synergistic effects are relatively low [21]. It appears that synergetic therapy, which combines more than one therapeutic strategy, can promote therapeutic potency when compared to sole treatment [26]. To address this drawback, the development of core–shell MOF structures can be used to promote a combination therapy strategy in cancer by utilizing the cooperative synergy of functional core and MOF-associated shell compounds [27,28]. One of the most well-studied examples is core–shell hybrid architectures, which can not only combine the novel characteristics of both the core and the shell compounds but also stimulate potential synergetic cancer therapeutics and imaging [27,28]. For example, different theranostic core-shell architectures with Fe_3O_4, Prussian blue (PB), Au, and manganese (Mn) as cores and MOFs as shells have been reported for efficient cancer theranostic [27–30].

There are several review papers on the application of MOF NPs for drug delivery [31,32], cancer therapy [33–37] and cancer theranostic [38–40]. For example, recently, Yang and co-workers [41] reviewed the application of core–shell NPs for photodynamic therapy (PDT)-mediated cancer therapy and imaging. However, to the best of our knowledge, there is no review on the application of core–shell inorganic metal NP@MOFs for cancer therapy. Accordingly, it seems that there is a room to overview the core–shell NPs of metal NP core and MOF shell for potential imaging-guided tumor therapy.

2. Synthesis of core–shell inorganic NP@MOF nanostructures

Even though the concept of binding metal ions to inorganic ligands dates back to 1964, the first simple MOFs were produced approximately in 1990. However, the term MOF was formalized in 1995 by Yaghi and co-workers [42] with the production of a Co-trimesate and then in 1997 by Kondo and co-workers [43] with the production of three-dimensional MOF nanostructures. Despite the wide range of MOF synthesis routes available, one of the most important strategies for the fabrication of core–shell inorganic NP@MOF nanostructures is the thermal-based chemical reaction approach. In this case, the molar ratio of materials, pH and solvent are considered as composition parameters, while time, temperature and pressure as process parameters. Since the traditional electrical small-scale method is time-consuming and expensive, MOFs are commonly produced using alternative synthesis methods such as microwave-assisted synthesis, electrochemical, mechanochemical, and sonochemical methods (Fig. 1). Despite combining these approaches with other chemical methods such as diffusion and deposition in the synthesis of inorganic@MOFs, the above approaches, which are based on direct synthesis and post-fabrication modifications, have faced serious challenges in commercialization of core–shell inorganic NP@MOF nanostructures (Table 1).

3. Magnetic NP@MOF nanostructures

MOF-based platforms can be used as potential candidates in the development of DDSs [29] as well as contrast agents for magnetic resonance imaging (MRI) [59]. In comparison to other systems for cancer therapy and imaging, the framework construction characteristics assure that core–shell MOFs not only provide a stimuli-responsive system as well as a center for large amounts of drug loading but also display promoted per-metal-relied relaxivity (Table 2). For example, Gd/thulium (Gd/Tm)-based MOFs can be used as pH-responsive drug delivery and dual-modal imaging contrast agents [60]. Drug loading and stimuli-responsive drug release can be engineered by modifying metal ions-based MOFs with a uniform shell and targeting moieties [60]. Also, these types of MOFs show sensitive magnificent longitudinal relaxivity [60,61].

However, the leaching of free ions causes cytotoxicity, which precludes their use in biomedical applications. Given that Mn^{2+} and Fe^{3+} ions show strong paramagnetic properties with much higher compatibility than Gd^{3+} ions, low toxic Mn- or Fe-based MOFs have been developed for potential cancer therapy [77,78] and MR contrast enhancement [79]. Despite the fact that the toxicity of Mn/Fe-based MOFs has been significantly reduced, ion release and moderate relaxivity still preclude their practical application as a potential system for potent cancer therapy and imaging sensitivity. To overcome these drawbacks and take advantage of the exceptional drug encapsulation potential of MOFs, the incorporation of NPs with distinctive magnetic features into MOFs can be considered as a useful strategy. The use of IONPs for immunotherapy and thermal cancer therapies is widespread [80,81]. Furthermore, various IONP formulations such as ferumoxsil, ferrixan and ferumoxide have already been used as biocompatible T2-MR contrast agents for clinical diagnosis. Several multi-functional core–shell-based IONPs for cancer diagnosis and therapy have recently been developed [82,83]. For example, Shen and co-workers [83] developed TiO_2-encapsulated Fe_3O_4 NPs (abbreviated as Fe_3O_4@TiO_2 NPs) to achieve targeted drug delivery and CT, where the shell not only serves as a sonosensitizer for sonodynamic therapy (SDT), but also uses as a platform for loading of chemotherapeutic (Fig. 2a). After fabricating Fe_3O_4 NPs (~200 nm) derived from $FeCl_3.6H_2O$, tri-sodium citrate and sodium acetate trihydrate by hydrothermal method, the TiO_2 shell was created by sol-gel method with a thickness of ~85 nm. Then, DOX was loaded by immersing the Fe_3O_4@TiO_2 NPs (371 nm) in the drug solution for 24 h. The fabricated platform showed simultaneous pH-dependent drug release as well as combined chemotherapy and SDT *in vitro*.

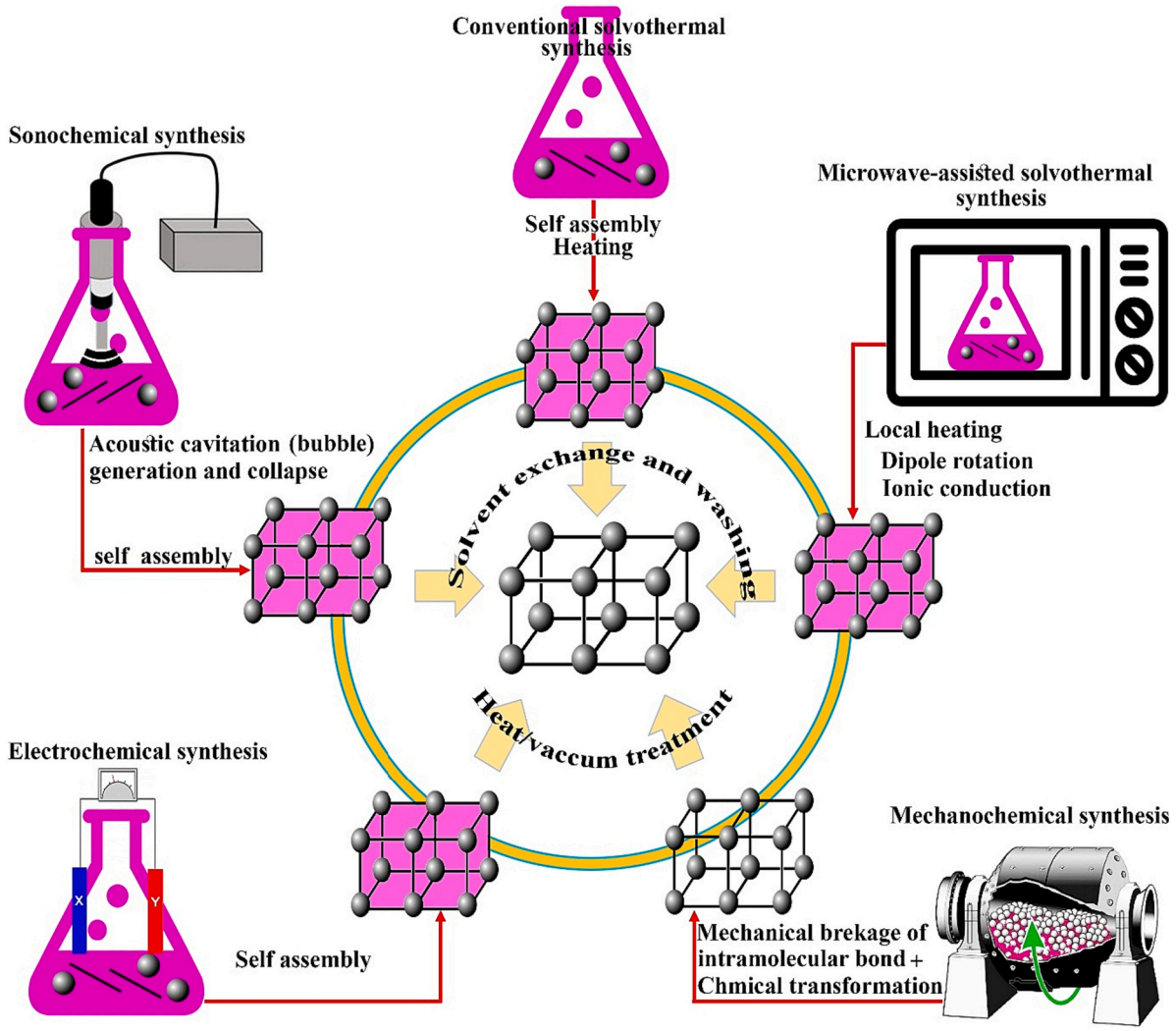

Fig. 1. Mechanisms of MOF synthesis based on thermal methods.

Thus, the constructed nano-platform with multi-functional characteristics serves as a potential system to selectively target cancer cells and display a sustained controlled release of combinatorial therapeutic payload in tumor cells with improved therapeutic potency and minimal adverse effects [83]. In addition to improving the biocompatibility and permeability of MCF-7 cells, the Fe_3O_4@TiO_2 NPs improved tumor treatment prospects by reducing the MCF-7 cells viability in a concentration-dependent manner as well as reducing the accumulation of the DOX in the kidney, heart and spleen tissues.

Furthermore, Rajkumar and Prabaharan [84] developed a potential core–shell Fe_3O_4@Au NP (Fe_3O_4@Au-DOX-mPEG/PEG-FA NP) with a diameter of ~18 nm for cancer theranostic. The developed platform had a saturation magnetization value of around 23 emu/g as well as a pH-sensitive drug release manner and improved cellular uptake in Hela cells due to the presence of hydrazone bond and FA, respectively (Fig. 2b) [84]. Also, following laser irradiation, the anticancer effect of the fabricated nano-platform was improved, which was mediated by the photothermal influence of the Au shell. Moreover, Fe_3O_4@Au core–shell NPs loaded with DOX have been used for potential MRI-guided magnetic targeted PTT-chemotherapy [85]. Because of the fact that PTT and MR imaging are available on these systems, they can be used for cancer theranostics. These findings indicated that IO-based core–shell NPs could be used as potential tumor-targeted DDSs with combined imaging, PPT and chemotherapy of cancer cells. For these reasons, it is rationally feasible to use magnetic IONPs to develop multifunctional MOF-based platforms with high relaxivity, improved target drug delivery and good biocompatibility. Zeolitic imidazolate frameworks (ZIFs) have been developed as multifunctional NPs with multiple and potential characteristics in cancer imaging and phototheranostics, either as pure ZIFs or as ZIF-based nanocomposites [86,87]. Among these promising materials, ZIF-8 has been investigated as a potential drug delivery carrier due to its rapid decomposition in an acidic environment [88,89], which benefits selective drug accumulation in mildly acidic tumor microenvironment (TME). The anticancer drug could be easily incorporated into the ZIF-8 shell, where IONPs can be used as the core platform to create a core–shell nanocomposite with diverse biomedical properties. For this purpose, Bian and co-workers [90] have designed multifunctional Fe_3O_4@ polyacrylic acid (PAA)/AuNPs/ZIF-8 NPs by layer-by-layer method with tri-modal cancer imaging and chemotherapy properties. After coating cetyltrimethylammonium bromide-modified Fe_3O_4 (25 nm) by polyacrylic acid, samples were immersed in a solution containing AuNCs modified with glutathione, ammonium, isopropyl alcohol solution of $Zn(NO_3)_2$, and 2-methylimidazole. Then, by stirring the final solution at 23 °C for 4 h, Fe_3O_4@PAA/AuNCs/ZIF-8 NPs with a dimension of 130 nm were produced. *In vitro* results in HepG-2 cells and *in vivo* outcomes on hepatoma-22 tumor-bearing mice showed that Fe_3O_4@PAA/AuNCs/ZIF-8 NPs improved the cancer treatment process through decreasing tumor volume in a concentration-dependent manner without causing toxicity in non-targeted tissues. The designed magnetic core–shell platforms not only provided tri-modal

Table 1
A summary of the production mechanism of inorganic NP@MOF nanostructures along with their advantages and disadvantages.

Class		Mechanism	Advantages/disadvantages	Samples	Shapes
Direct synthesis (one-pot)	Conventional	Proper mixture of precursors including ligands and metal ions in a thermal reservoir	**Advantages**: Simplicity, high commercialization probability, cost-effective **Disadvantages**: Lack of control on the metal distribution, the probability of the presence of one metal in the nodes	Al/Fe-ITQ-NO_2 [44], Zn/Mg-MOF-74 [45], MIL-101(Al/Fe)–NH_2 [46]	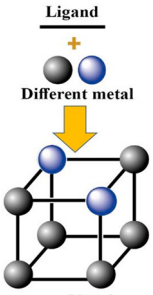
	Metalloligand	Using ligands that contain a second metal complex (metalloligand) compatible with MOF synthesis	**Advantages**: A simple process, cost-effective, high stability **Disadvantages**: The presence of two different metal sites in the network and connecting nodes, create new cavities with new properties	Zr[PCN-161-$CoCl_2$] [47], (Mn.Fe.$O)_2$(TCPP-$Ni)_3$ [48]	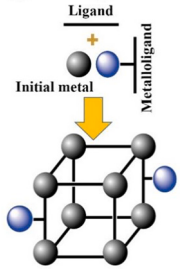
	Epitaxial growth	The metal ions growth on the MOF surface including MOF shell with M2 metal on the MOF core with M1 metal	**Advantages**: Tunable shell thickness and core diameter, possibility to integrate different crystal structures based on metal ions **Disadvantages**: Multi-steps, limited commercialization	ZIF-8-on-In-dpda [49], MOF-5@IRMOF-3 [50]	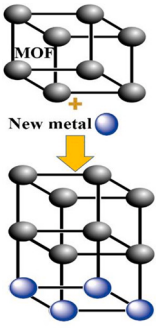
Post-synthetic modification	De- and *Re*-metalation	Creation of vacancies by metal removal and incorporation of new metal into MOFs	**Advantages**: The use of new metals that did not have the possibility to be present in the MOF manufacturing process **Disadvantages**: Multi-steps, lack of complete control over the output of metal ions in different areas	$[Cu(CH_3CN)_4]BF_4$ [51], Mn^{III}SO-MOF [52]	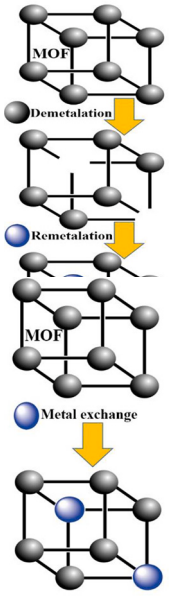
	Metal exchange	Exchange is done based on the control of concentration, time and temperature parameters causing the selective replacement of the initial metal with the selected metal with stirring the solution	**Advantages**: Relative control of the selective metal concentration introduced in the lattice, the use of special metals without interference in the initial MOFs synthesis **Disadvantages**: Multi-steps, randomly structure without any site-specificity, high solubility under reaction conditions	TMU-22(Zn/Co) [53], Ni/Zn-MOF-5 [54], Zr-MOF-RhCL [55]	

(*continued on next page*)

Table 1 (*continued*)

Class	Mechanism	Advantages/disadvantages	Samples	Shapes
Metal insertion	Attachment of a new metal through cation/anion exchange or using functional groups such as thioeter in MOFs	**Advantages**: High selectivity and affinity by new metal with free valence **Disadvantages**: Multi-steps, occupying the pore space, lack of uniform distribution of secondary metal, poor stability	MOF-253-Pt [56], UiO-67-ox-Cu [57], UiO-67-bpy-(Ni or Cu or Fe) [58]	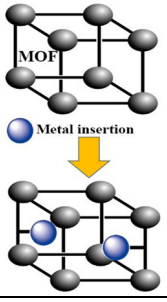

imaging and chemotherapy, but also they displayed a large drug payload, pH-sensitive drug release, good biocompatibility, and feasible separation enabled by magnetic strategy [90]. The induced aggregation-enhanced fluorescence mediated by Zn^{2+} released from ZIF-8 and isopropanol interferes with the hydration shell of AuNPs can play a key role in the fluorescence imaging of cancer cells enabled by Fe_3O_4@PAA/Au/ZIF-8 NPs. On top of that, the IONPs and AuNPs integrated in these systems act as contrast agents in MRI and CT scan, respectively [90]. Moreover, Chowdhuri and Bhattacharya [63] designed a core–shell MOF platform based on Rhodamine B isothiocyanate (RITC)-IO@porous isoreticular (IR)MOF-3/FA NPs, which superparamagnetic Fe_3O_4 NPs were employed as bimodal MRI and fluorescent contrast agents, as well as magnetically guided drug delivery nanocarriers.

However, the poor colloidal stability of IRMOF-3 and the low biocompatibility of Zn-based MOF stemming from the membrane/DNA damage triggered by the competition of ions preclude their feasible utilization in biomedicine [91,92]. Furthermore, the synthesis approaches typically include several steps, and the capacity of MOF-based nanocomposites in imaging and drug delivery, as well as the cytotoxicity, should be explored further *in vivo*. Therefore, additional investigation on MOF-based theranostic agents with feasible synthesis routes and good biocompatibility seems necessary and of great importance. For this reason, Zhao and co-workers [64] incorporated magnetic NPs with MOF UiO-66 showing high chemical and colloidal stability to synthesize potential theranostic MOF core–shell nanocomposites (Fe_3O_4@UiO-66) with a dimension of 150 nm to achieve MR imaging and drug delivery *in vitro* and *in vivo* (Fig. 3a). Also, the presence of Zr—O clusters, as well as numerous porous structures, metal active sites, and hydrophilic features, make UiO-66 suitable for the absorption and release of DOX, which is dependent on the strong coordination forces between the OH groups in drug and Zr(IV) centers in MOF platform. Thus, Fe_3O_4@UiO-66-DOX core–shell nanocomposites were fabricated using a facile *in situ* growth strategy, and they simultaneously provided the T2-MR contrast and drug delivery capability originating from the Fe_3O_4 cores and MOF shells, respectively [64]. In general, the fabricated Fe_3O_4@UiO-66-DOX core–shell nanocomposites improved tumor treatment by reducing HeLa tumor volume in a dose-and time-dependent manner (from 5 to 100 mg/L over 24 and 48 h) while also improving MR imaging capability.

To target cancer cells, different functional ligands such as FA, antibodies and aptamers (Apts) have been widely attached to the surface of NPs [93]. For example, Alijani and co-workers [94] developed magnetic Fe_3O_4@MOF-DOX-carbon dots (CDs)-Apt with a dimension of ~16 nm for imaging and drug delivery . They loaded Fe_3O_4@MOF nanocomposites with DOX followed by conjugation to CDs with highly fluorescent properties and capping with Apt targeting nucleolin, AS1411. In comparison to normal cells, the Fe_3O_4@MOF-DOX-CDs-Apt nano-conjugates were able to selectively provide pH-sensitive drug release to nucleolin-upregulating tumors with improved therapeutic outcomes against MDA-MB-231 human breast cancer cells. Also, the carrier showed promising fluorescence imaging functionality enabled by CDs to potentially monitor the bio-distribution of the NPs [94].

Besides, the incorporation of switchable host-guest systems on the surface of drug carriers, such as nanovalves, can play an important role in controlling the release of loaded drugs [96], the advancement of the developed nano-platform with a "turn-on/off" capability under unique TME, an improved therapeutic potency, and reduced adverse effects of chemotherapeutics [97,98]. However, the fabrication strategy for such intelligent systems is still in its infancy, particularly in terms of incorporating gatekeepers and the construction of well-defined MOF structures [95]. To address the integration of nanovalves, pillararenes as synthetic macrocycles with potential benefits over other comparable compounds have received much more attention for their advancement in the field of stimuli-sensitive drug delivery. These compounds can serve as promising gatekeepers to manipulate the controlled release of payloads by regulating the formation of host–guest complexes to form stalk-mimic structures on MOF [99,100]. As proof-of-concept investigations, water-soluble pillararenes such as pillar [5] arene derivatives have been widely used and proven to act as smart nanovalves to respond to on-command drug release [101–104]. Inspired by these facts, Wu and co-workers [95] designed a multimode theranostic core–shell magnetic MOF nano-conjugate with a dimension of ~89 nm based on pillararene-derived gatekeepers. They developed a smart theranostic carboxylatopillar [6] arene (WP6)-modified magnetic UiO-66 Zr-MOF (Fe_3O_4@UiO-66@WP6) through *in situ* growth method mediated by core–shell structure, with the ability to endow TME-induced drug release, MRI capability, as well as promising chemotherapy (Fig. 3b) [95]. Meanwhile, Fe_3O_4@UiO-66@WP6 demonstrated biocompatibility and anticancer effects on HUVEC and HeLa cells *in vitro*, respectively, which is a promising therapeutic approach for cancer treatment. Therefore, Fe_3O_4@UiO-66-NH_2, WP6 and 5-fluorouracil (5-FU) were used as MRI tracers, manipulating drug release (nanovalves) and chemotherapeutic agents, respectively. In other words, it can be claimed that the core and shell endow the complex with the capability of simultaneous imaging and targeted drug delivery-based cancer therapy, respectively. Tightness-controllable supramolecular gatekeepers (pseudorotaxanes) can be used in the development of intelligent multistimuli-responsive DDSs [105,106].

Furthermore, dihydroartemisinin (DHA) and artesunate (AS) derivatives have been shown to induce oxidative stress mediated by ferrous [Fe (II)] ions. Nevertheless, the low levels of Fe (II) in cancer cells preclude the potent anticancer effects of DHA [107]. As a result, transferrin (Tf)-based DDSs have been developed to transport AS [108] and DHA [109] for cancer therapy *in vivo*. However, the synthesis procedures of those DDSs are so complicated thus hindering their biomedical implementations. These facts led to a great deal of interest in introducing new approaches to increase Fe availability in cancer cells. MIL-100(Fe) is a promising MOF platform for biomedical applications due to its strong interaction with payloads, good biocompatibility and biodegradability [110]. Additionally, hydrophobic interactions between anticancer drugs and host [MIL-100(Fe)] can further enhance drug loading. Considering its low cytotoxicity and *in vivo* biodegradability, MIL-100(Fe) appears to be a promising co-delivery system for Fe and

Table 2
Characteristics and performance of magnetic, Qds, Au and Gd MOFs in tumor therapeutics .

Class	Name	Research method	Application and outcomes	Ref.
Magnetic@MOF nanostructures	MIL-101-NH_2(Fe)@SiO_2 @c(RGDfk)	Drug carrier: Cisplatin Targeted cell: HT-29 Method: *In vitro* Size: ~200 nm	Chemotherapy: Stopping tumor cell growth, dose-dependent toxicity, enhancing drug permeability, reducing burst drug release	[62]
	Fe_3O_4@IRMOF-3@FA-RITC	Drug carrier: Paclitaxel Targeted cell: HeLa cell Method: *In vitro* Size: ~100 nm	Chemotherapy: Sustained drug release without burst release, dose-dependent mortality of cancer cells, low toxicity in healthy cells, increased drug permeability.	[63]
	Fe_3O_4@UiO-66	Drug carrier: Doxorubicin (DOX) Targeted cell: HeLa Method: *In vitro* + *In vivo* Size: ~150 nm	Chemotherapy + imaging: Sustained and effective drug release, high mortality of cancer cells, significant inhibition of tumor size, low biocompatibility, low toxicity and improved imaging quality.	[64]
	Fe_3O_4@C@MIL-100(Fe)	Drug carrier: Dihydroartemisinin Targeted cell: HeLa Method: *In vitro* + *in vivo* Size: ~190 nm	Chemotherapy + imaging: Sustained drug release, high toxicity in cancer cells, reduction of tumor volume, non-toxicity in the major tissues, increase in imaging quality and stability up to 24 h, enhancing intracellular ROS.	[30]
	MIL-100(Fe)	Drug carrier: Curcumin Targeted cell: HeLa Method: *In vitro* + *in vivo* Size: 220–550 nm	Chemotherapy + photothermal therapy (PTT): pH-dependent drug release, high toxicity in cancer cells, improved cell permeability, increased apoptosis, reduced tumor volume, enhancing local temperature up to 50 °C in tumor tissue.	[65]
	HA/Ara-IR820@ZIF-8	Drug carrier: Cytarabine Targeted cell: 4 T1 Method: *In vitro* + *in vivo* Size: ~120.5 nm	Chemotherapy + PTT: Reducing the growth of cancer cells, pH-responsive drug release, reducing tumor volume, modulating the EPR effect, lack of toxicity in the major tissues.	[66]
	NH_2-MIL-125	Drug carrier: DOX Targeted cell: MCF-7 Method: *In vitro* Size: ~300 nm	Chemotherapy + PDT: Good compatibility, dose-dependent toxicity in cancer cells, sustained drug release without burst release, improved drug permeability, increased intracellular ROS.	[67]
	Fe-soc-MOF@PEG-NH_2-ICG	Drug carrier: DOX Targeted cell: HeLa Method: *In vitro* + *in vivo* Size: ~220 nm	Chemotherapy + PTT + PDT + imaging: Dose-dependent toxicity, induction of apoptosis and intracellular ROS, reduction of tumor volume, non-toxicity in the major tissues, improvement of MR imaging, effective combination of PTT and PDT.	[68]
Quntum dots@MOF nanostructures	Cu-TCPP	Targeted cell: Saos-2 Method: *In vitro* + *in vivo* Size: ~330 nm	PTT + PDT + imaging: Increase of single oxygen, enhancement of apoptosis, increase of MR imaging quality, reduction of tumor volume, significant increase of intracellular temperature with PTT.	[69]
	DOX/AS1411@ PEGMA@GQDs @γ-CD-MOF	Graphene QDs (GQDs): Drug carrier: DOX Targeted cell: MCF-7 Method: *In vitro* + *in vivo*	Chemotherapy + imaging: pH-responsive controlled release of drug, reduction of tumor volume, inhibiting tumor cells growth, the ability to monitor drug penetration based on QD optical activity, non-toxicity on the major tissues.	[70]
	DOX-ZIF-8/GQD	GQDs: Drug carrier: DOX Targeted cell: 4 T1 Method: *In vitro* + *in vivo* Size: 50–100 nm	Chemotherapy + PTT + imaging: Dose-dependent toxicity, pH-responsive controlled drug release, monitoring drug penetration.	[71]
	BQMIL@cat-fMIL	Black phosphorus QDs (BPQDs): Drug carrier: Cyanine 3-labeled caspase peptide Targeted cell: HeLa Method: *In vitro* + *in vivo* Size: ~60 nm	Chemotherapy + PTT + PDT + imaging: Reduction of tumor volume, reduction of hypoxia, increase of apoptosis	[72]
	PEG-Au/FeMOF @CPT	Drug carrier: Camptothecin Targeted cell: HepG2 Method: *In vitro* + *in vivo* Size: 30–120 nm	Chemotherapy: Induction of cellular starvation by glucose degradation, increased $^{\bullet}OH$, decreased tumor volume, dose-dependent toxicity, increased intracellular ROS, and potential drug release behavior.	[73]
Au NP@MOF nanostructures	MIL-101(Fe)@BSA-AuNCs	Targeted cell: HepG2 and H22 Method: *In vitro* + *in vivo* Size: 150–261 nm	PTT + imaging: Increasing MRI and FI imaging quality, decreasing tumor volume, increasing free radicals in tumor cells, biocompatibility in off-target cells, decreasing tumor cell viability.	[74]
	Au@ZIF-8/DOX	Drug carrier: DOX Targeted cell: HeLa Method: *In vitro* + *in vivo* Size: 200 nm	Chemotherapy + PTT + imaging: Increasing drug permeability in cancer cells, reducing the cancer cell viability percentage, enhancing cumulative heat in PTT, reducing tumor volume, non-toxicity in the major tissues, increasing the quality of PA imaging.	[75]
	Gd@MOF- PNIPAM-co-PNAOS-co-PFMA	Targeted cell: FITZ-HSA Method: *In vitro* Size: 100–150 × 20–25 nm	Imaging: High biocompatibility and increased imaging quality	[76]

drugs. Magnetic IONPs can also be used as a core to develop magnetically guided theranostics. T2 contrast agents reduce the confusion associated with endogenous signals that appear dark in MR images when used in conjunction with MR imaging. Furthermore, two-photon fluorescence imaging enabled by CDs can provide several advantages such as low cross-section, high tissue penetration and improved resolution. Hence, CDs have sparked a lot of interest in ultrasensitive imaging of cancer cells as well as visual monitoring of DDSs [30]. Hence, Fe_3O_4@C@MIL-100 (Fe) NPs with a dimension of ~190 nm were synthesized by layer-by-layer method from Fe_3O_4@C (core) and MIL-100

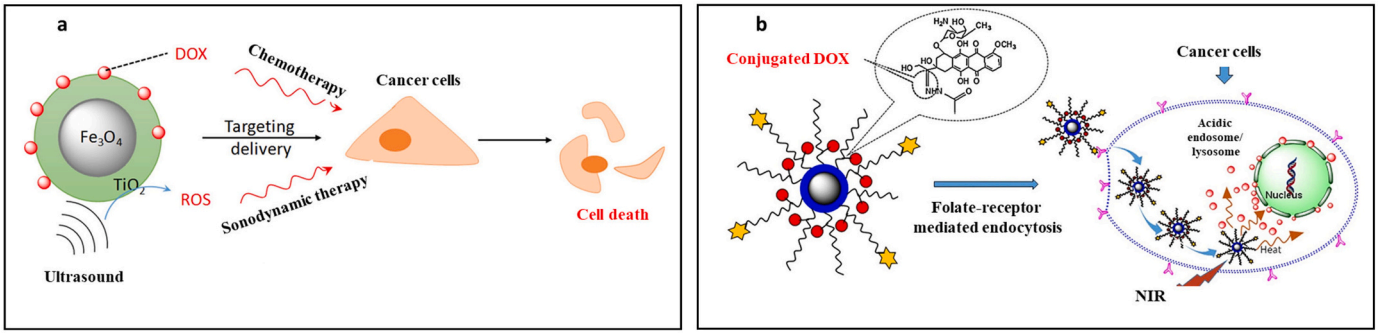

Fig. 2. (a) *In vitro* targeted chemo-SDT of cancer cells using core–shell IO@TiO_2 NPs [83]. (b) Schematic illustration of the multi-functional core–shell IO@Au NPs for cancer therapy [84].

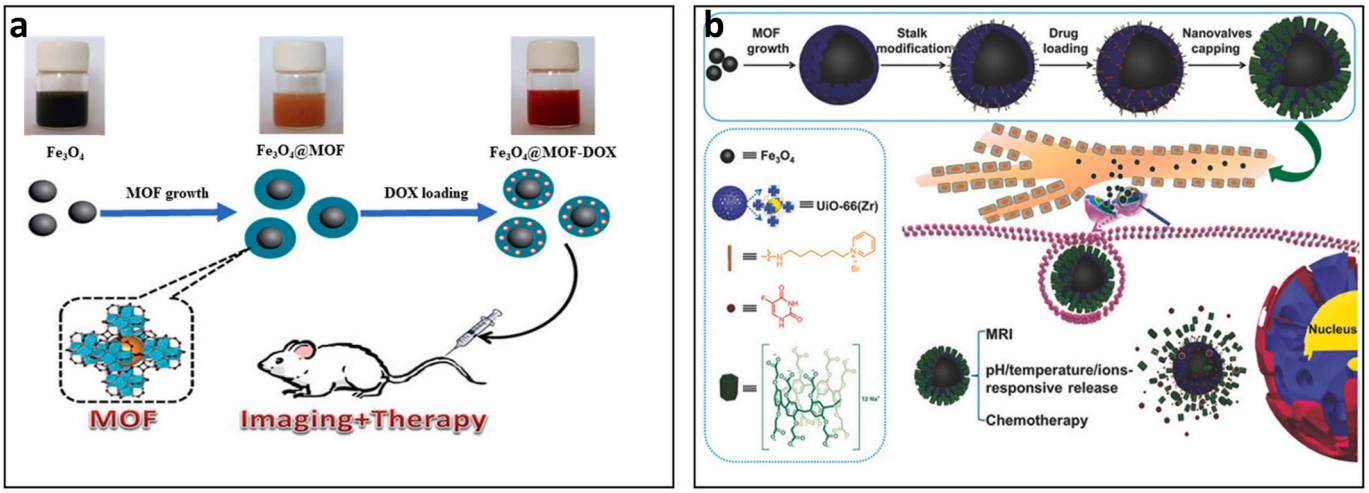

Fig. 3. (a) Simultaneous MRI and drug delivery using theranostic MOF core–shell Fe_3O_4@UiO-66 nanocomposites [64]. (b) Stimuli-sensitive core–shell Fe_3O_4@UiO-66 nano-conjugates incorporated with @carboxylatopillar [6] arene (WP6) nanovalves [95].

(Fe) shell with ~40 nm thickness with a magnetic targeting capability. The carbon layer with integrated CDs was shown to act as a two-photon fluorescence imaging agent. After exposure to acidic TME, the shell layer degrades, resulting in the simultaneous release of DHA and Fe (III) ions, the latter of which is reduced to the Fe (II) state by reductive capacity of the cell [30]. Eventually, Fe (II) reacts with DHA, producing high levels of cytotoxic ROS, resulting in a 4- to 6-fold decrease in tumor volume and a 40% decrease in HeLa cell viability (dose-dependently: 25–100 μg/mL). Thus, as-prepared Fe_3O_4@C@MIL-100(Fe) NPs may exhibit dual-modality imaging of cancer cells as well as pH-sensitive drug and Fe ion release manipulated by an external magnetic field, making them potential candidates for cancer theranostics.

Also, the application of core–shell dual (CSD) MOFs can combine dual-modality imaging along with single or combined cancer therapy. In this line, Wang, Zhou [111] developed a smart theranostic core–shell nano-platform based on $Mn_3[Co(CN)_6]_2$@MIL-100(Fe) MOFs (CS-MOFs) embedded with AS anticancer drug for highly effective pH-sensitive/Fe-mediated cancer therapy along with multimodality imaging. In this approach, after fabricating the central core ($Mn_3[Co(CN)_6]_2$) with a dimension of 150 nm, the biodegradable MIL100(Fe) shell was grown through the layer-by-layer method with alternating deposition of H_3BTC and FeCl3 on the core surface. They showed that a number of coating cycles affects the morphology and size of porous nanostructures. In physiological pH 7.4, CS-MOFs could not release AS, but at acidic pH 5.0–6.5 a significant sustained drug release was observed, presumably due to possible decomposition of the outer MIL-100(Fe) shell. Over and above that, the reduced Fe (II) ion reacted with AS to result in the formation of high levels of carbon-centered radicals and ROS in cancer cells, which cause HeLa cell death and decreased tumor volume [111]. Also, due to the presence of hybrid materials dual-modal imaging (MRI and two-photon luminescence) was achieved. A potential strategy for imaging-guided tumor-specific therapy can be achieved by heterogeneous hybridization of dual MOFs with different properties for drug delivery and dual-modality imaging. Furthermore, Wang and co-workers [112] developed a multifunctional PB-MOF@MIL-100(Fe) CSD-MOFs nano-platform with a dimension of 190 nm through a layer-by-layer method on the cubic core (PB: at around 90 nm), which served as a potential dual-model imaging-guided combinational cancer therapy. Also, the inner PB-MOF core and the outer MIL-100(Fe) MOF shell could serve as T1/T2 and T2 MRI contrasting agents, respectively. It was also shown that, compared to CDs, PB-MOF@MIL-100(Fe)CSD-MOF NPs not only act as a fluorescence optical imaging agent but also significantly reduce tumor volume without causing toxicity in major tissues mediated by increasing Artemisinin permeability and inducing toxicity. As a result, the use of dual-model imaging-guided combinational cancer therapy was discovered to provide complementary diagnostic outcomes and synergistic benefits over single modality-mediated theranostics (Fig. 4). Recently, based on the layer-by-layer method, multifunctional core–shell hybrids of copper sulfide@MOF NP (HCuS@MIL-100) were fabricated [113]. HCuS@MIL-100 NPs outperformed conventional cancer therapeutic and diagnostic methods by improving PTT effects with HCuS as a NIR-II photothermal agent and T2 magnetic resonance imaging with MIL-100 as a contrast agent [113].

The CSD-MOFs were highly loaded with a hydrophobic anticancer

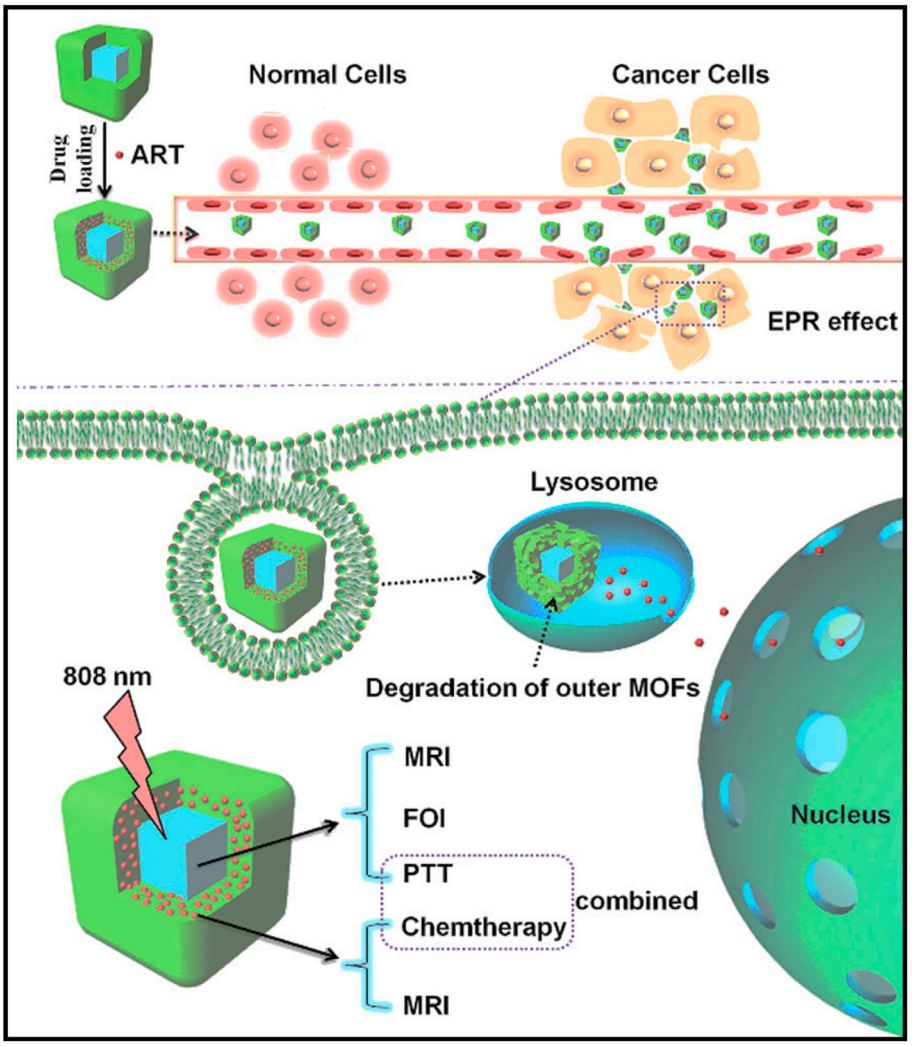

Fig. 4. Core-shell dual (CSD)-MOF NPs, PB-MOF@MIL-100(Fe), for pH-sensitive artemisinin (ART) delivery, MR and optical dual-model imaging-guided combinational treatment of cancer [112].

drug, artemisinin (ART), which was able to be released in acidic TME in a pH-sensitive manner. Moreover, the combination of PTT and chemotherapy was achieved both *in vitro* and *in vivo* when ART was incorporated with CSD-MOFs [112]. Theranostic CSD-MOF nanostructures even without targeting agents are generally considered safe cancer therapeutics because of their good biocompatibility and low side effects. In this line, CSD-MOFs@DOX composed of PB and ZIF-8 can be used for dual-modality imaging as well as combined PTT and chemotherapy [112]. PB incorporated onto the surface of MOF can also be developed as a hybrid material for combined cancer therapy [114]. Gao and co-workers [114] found that UIO-66-NH_2/PB can serve as a potential pH-responsive drug carrier capable of stimulating PTT following the exposure of NIR light as well as catalytic activity toward the endogenous H_2O_2 to overcome hypoxia in cancer cells [114].

4. Quantum dots@MOF nanostructures

The combination of QDs and MOFs, either as smart shells or cores, allows for the manipulation of controlled drug release, PTT and imaging (Fig. 5, Table 2). Based on their promising optical properties, functional fluorescent NPs such as semiconductor QDs, have been exhibited to provide potential applications in bioimaging and therapy [115,116]. However, semiconductor QDs do not show biocompatibility stemming from the heavy metal components and their large size, which results in corresponding interaction with the intracellular performances [117].

Carbon QDs (CQDs) are known as small carbon NPs with a typical size of <10 nm, which show several benefits over classical semiconductor QDs, including high colloidal stability and good biocompatibility, making them particularly potential for dual/multi-modality treatment of cancer. The potential chemiluminescence properties of CQDs derived from their unique electronic characteristics (electron donors and acceptors) ensure they have extensive capacity in chemiluminescence-guided cancer therapy [118]. For this reason, He and co-workers [119] fabricated CQD@ZIF-8 nanocomposite with a dimension of 110 nm through an encapsulation process and employed it for simultaneous drug delivery and imaging (Fig. 6a). Hydrophilic green-fluorescent CQDs (λ_{ex} = 365 nm; λ_{em} = 497 nm) (Fig. 6b) were successfully encapsulated as a core in a ZIF-8 platform with highly yielded optical features, and the resulting nanocomposites were subsequently loaded with 5-FU. The *in vitro* drug release assays at pH values of 7.4 and 5.5 revealed 67% and 92% drug release, respectively, revealing the pH-sensitive drug delivery behavior of CQD@ZIF-8. The *in vitro* cytotoxicity assay of CQD@ZIF-8 against Hela, DU145 and L929 cells indicated that core–shell CQD@ZIF-8 nano-conjugates were biocompatible up to a concentration of 25 μg/mL. After 24 h of incubation with CQD@ZIF-8-5-FU, imaging analysis revealed an apparent green fluorescence in the cytoplasm caused by NP cellular uptake. This study demonstrated that QD@MOF nanocomposites have the potential to be

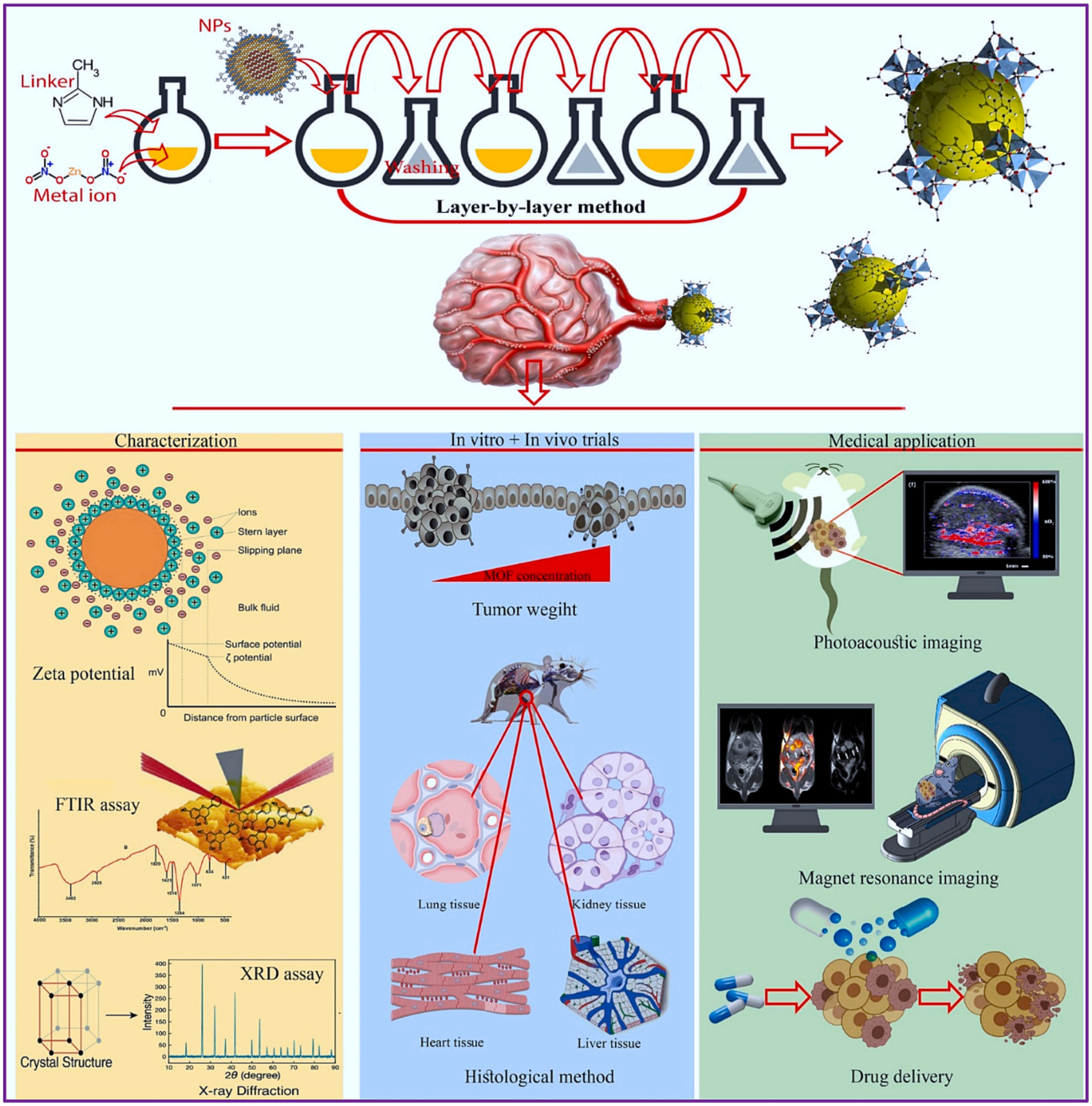

Fig. 5. A schematic illustration of the synthesis and application of core–shell@MOF NPs in tumor therapy and imaging.

used in theranostic applications [119].

In another study, GQDs demonstrated potential NIR absorbance, promising PTT and good biocompatibility *in vivo* [120]. Additionally, the presence of different groups on GQDs makes them appealing for grafting with various types of NPs. For example, Tian and co-workers [71] developed a multifunctional system for synergistic chemo- and PTT using a simple one-pot approach, in which ZIF-8 and embedded GQDs served as drug carriers and local photothermal parts, respectively (Fig. 6c). The outcomes indicated that ZIF-8/GQD NPs with good colloidal stability and with a narrow particle size ranging from 50 to 100 nm were able to encapsulate DOX and stimulate controlled drug release and cell cytotoxicity under NIR irradiation for 3 min . *In vitro* results showed the high toxicity of DOX-ZIF-8/GQD NPs on 4 T1 cells through a synergistic effect mediated by chemotherapy and PTT under NIR radiation. Hence, ZIF-8/GQD NPs can be promising versatile nanocarriers for synergistic breast cancer therapy [71].

However, MOF NPs and their syntheses have been linked to varying degrees of cytotoxicity, either from metal ion release or organic groups, which precludes their use in biomedicine. Using various polymers such as PEG, poly-L-lactide, poly(glycidyl methacrylate), and poly-N-isopropylacrylamide with MOF NPs *via* "amidation and click-modulation" can thus be a useful strategy to improve NP biocompatibility [121–123]. Based on this fact, a hydrophilic comb-like architecture of the PEG methacrylate (PEGMA) was reported to mitigate the cytotoxicity of MOF-based NPs [70,124]. Moreover, because γ-cyclodextrin (γ-CD) is a natural product commonly used in the synthesis of MOFs, the

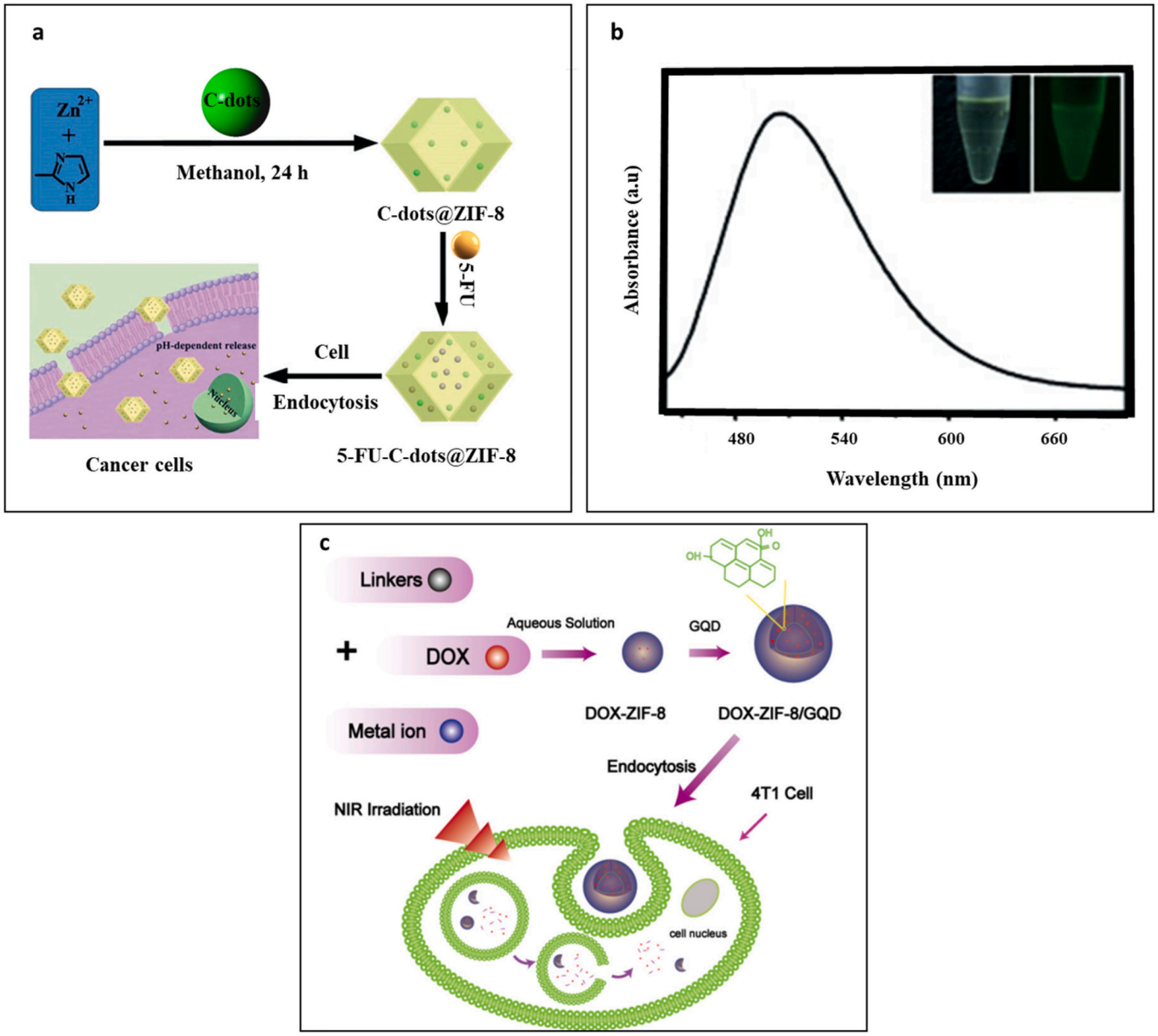

Fig. 6. (a) Schematic representation of the synthetic route of the CQD@ZIF-8 for simultaneous drug delivery and fluorescence imaging of cancer cells [119]. (b) photoluminescence spectrum of CQDs [119]. (c) Synergistic chemo- and PTT using MOF/GQD NPs [71].

developed CD-MOFs are prone to decomposition or dissolution after incubation in bio-fluids, and thus improving their colloidal stability is highly desired for biological applications. Although some post-synthetic modifications can overcome this disadvantage [125,126], the transition of crystalline structures to cubic gels typically occurs upon biomedical applications of CD-MOFs. In this context, a functional strategy is demanded to graft a biopolymer on the inorganic surface of MOFs. It seems that PEGylation can be widely utilized for surface functionalization of MOFs in order to inhibit the non-specific protein corona formation. Furthermore, PEGMA as a pH-sensitive segment can be obtained by manipulating polymerization by surface-initiated atom transfer radical polymerization (SI-ATRP) [127], a typical method for grafting biopolymers on the surface of inorganic NPs [128]. Consequently, the modification of the γ-CD-MOF with some biopolymers such as PEGMA through SI-ATRP can be used as a propitious approach to advance novel DDSs. Moreover, γ-CD-MOF embedded with GQDs can hold great promise for early cancer imaging [129]. Based on this knowledge, Jia and co-workers created a core-shell GQDs@γ-CD-MOF NP with dimensions of 300 to 900 nm that was functionalized with PEGMA *via* SI-ATRP for drug delivery and cancer therapy [70]. It was discovered that modifying NPs with a PEGMA layer can result in the formation of a pH-responsive structure with improved colloidal stability and lower cytotoxicity [70]. Also, GQD was used as a fluorescent probe to detect the bio-distribution of DDSs in the subcellular compartments [Fig. 7(i)]. In addition, a proof-of-concept study of *in vitro* drug delivery determined the promoted tumor-targeted drug delivery [70]. Based on the interaction of the AS1411 Apt and nucleolin, the designed nanocarrier found a gateway into tumor cells mediated by endocytosis, with the well-planned release of DOX stimulated through a pH-sensitive manner in TME. Although the developed core–shell nano-platform did not cause significant cytotoxicity on MCF-7 cells at concentrations ranging from 0 to 50 μg/mL, the use of DOX/AS1411@PEGMA@GQDs@γ-CD-MOF NPs resulted in a significant decrease in MCF-7 cell viability and tumor volume without body weight loss [Fig. 7(ii)] and toxicity in the major tissues through increasing DOX permeability in cancer cells.

BPQDs with a size of <10 nm also have several advantages over

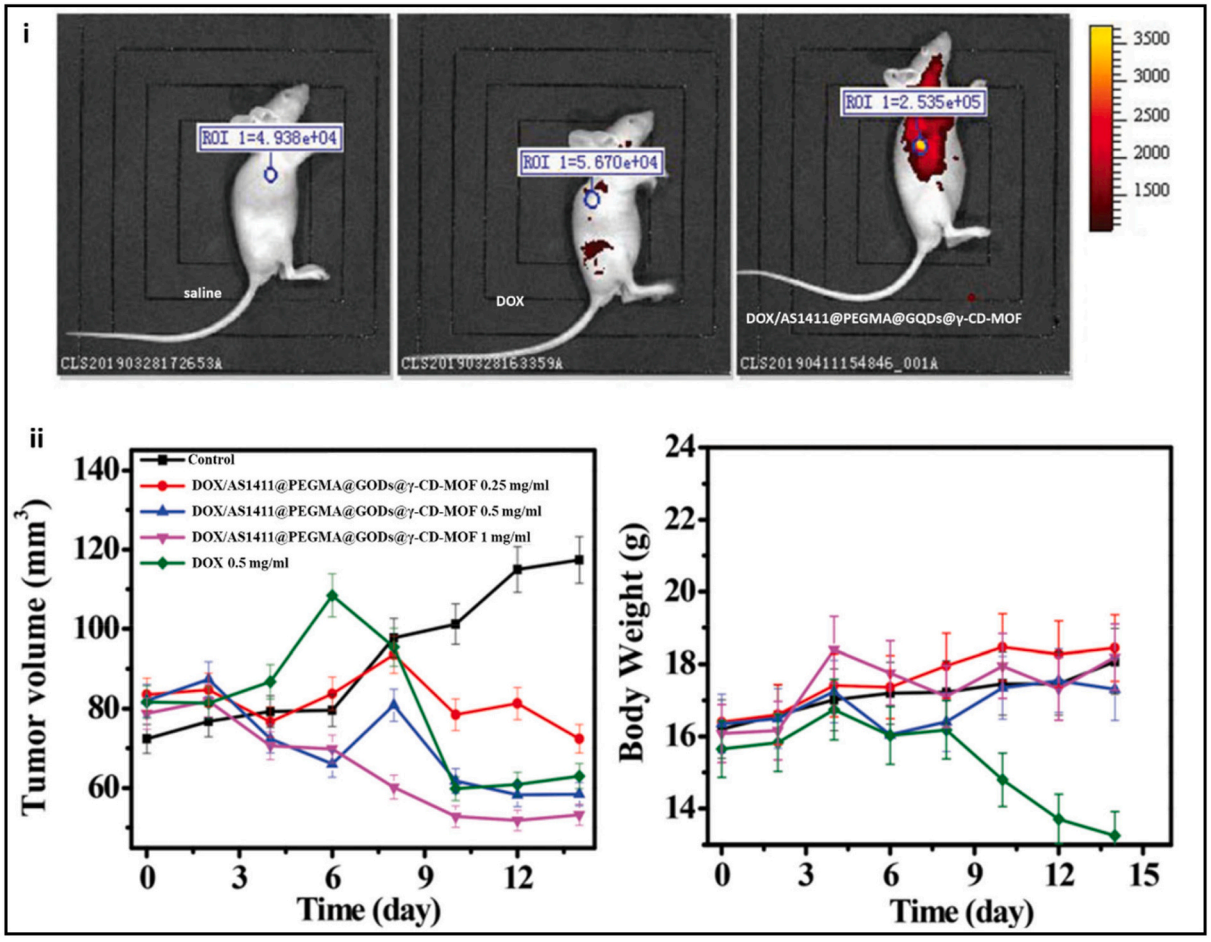

Fig. 7. *In vivo* imaging of MCF-7 tumor-bearing mice injected with different samples (i), tumor volume growth curves and body weight change of the mice (ii) [70].

classical semiconductor QDs comparable to CQDs. Thus, Du, Qin [130] by the introduction of framework exchange and application of MOFs (Cu-ZIF-8) (45 nm), BPQDs (2 nm) and S-nitrosoglutathione (GSNO) as a nitric oxide precursor were potentially able to encapsulate negatively-charged BPQDs into ZIF-8 [HKUST-1@MIL-100(Fe) (BHM)] [130]. They found that electrostatic forces can play a key role in the interaction of BPQDs with ZIF-8, and only negatively-charged QDs can be encapsulated in the ZIF-8 structure. The TME (acidic environment and high GSH level) along with stimulating the generation of ·OH and NO from H_2O_2 and GSNO, respectively catalyzed by reduced Cu^+ and Fe^{2+}, could result synergistically in the induction of apoptosis and a significant reduction in the number of viable SGC-7901 cells and tumor volume

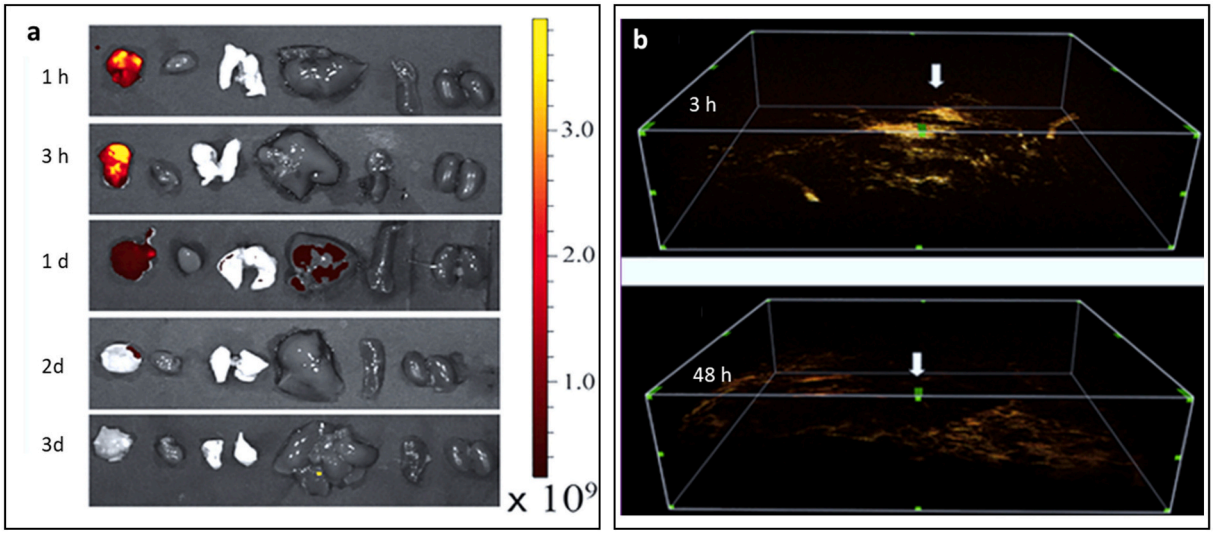

Fig. 8. (a) *Ex vivo* images of tissues in SGC-7901 tumor-bearing nude mice after intravenous injection of nitrosoglutathione (GSNO)-(HKUST-1@MIL-100(Fe) (abbreviated as G(c-BHM) [130]. (b) The 3D perspective of photoacoustic (PA) images of tumor zone [130].

[130]. Then, it should be indicated that hyperthermia induced by illumination of near IR (NIR) accelerates the formation of free radicals, a photo-reduction reaction mediated by MOF [130]. It was also seen that the fluorescence intensity increased with the selective accumulation of the G-BHM and the reduction of Fe^{3+} and Cu^{2+} ions mediated by GSH as evidenced by *ex vivo* images (Fig. 8a). The degradation of G-BHM over time can also be determined by measuring the photoacoustic (PA) response of BPQDs (Fig. 8b) [130].

Because of the quantum confinement and edge effects, BPQDs have been shown to possess several promising optical characteristics, including singlet oxygen ($^1O_2$) production and photothermal conversion potency for PDT and PTT, respectively [131,132]. In addition, to develop a potential cancer therapeutic structure against hypoxic tumor cells, the simultaneous integration of NPs and oxidative enzymes in MOF NP structures may be a feasible strategy to inspire researchers to develop a programmable system for cancer therapy. Therefore, Liu and co-workers [72] developed a BPQD and catalase co-encapsulated MIL-101 heterostructure (BPQD-MIL@cat-MIL) for enhanced cancer therapy in hypoxia (Table 2) [72]. Interestingly, the integrated MIL-101 system was used as a tandem biocatalyst to convert intracellular H_2O_2 to O_2 enabled by catalase, followed by injection of O_2 into BPQD inner layer, causing a high quantum yield of $^1O_2$. Following endocytosis, the BPQD-MIL@catalase-MIL NPs demonstrated a nearly 9-fold increase in PDT potency compared to those without catalase. As MIL-101 is known as an acid-resistant type of MOF, it can protect catalase from pH-induced denaturation and supply abundant O_2 for BPQDs-based PDT. Furthermore, a combination therapy was achieved *in vitro* and *in vivo* by coupling with the PTT of BPQDs [72]. Hence, it was concluded that layered acid resistance MIL-101-based NPs integrated multiple performances for successful treatment against hypoxic environments.

5. Gold NP@MOF nanostructures

As a unique type of metal nanomaterial, AuNPs display exceptional characteristics in imaging and therapeutics based on surface-enhanced Raman scattering and photoacoustic along with PTT (Table 2) [133]. Anisotropic AuNPs show two different plasmon absorptions in the visible and NIR regions [133]. The NIR region's absorption makes anisotropic AuNPs ideal photothermal agents because of the deep tumor penetrating properties of the NIR region [134,135]. The photothermal performance of anisotropic AuNPs is triggered by a NIR-808 laser-mediated localized surface plasmon resonance, and several reports have already overviewed this phenomenon [136–138]. Also, anisotropic AuNPs are known as bio-stable agents that do not decompose easily and provide an improved scattering signal , making them potential contrast agents [139]. Therefore, it is expected that AuNPs can show improved theranostic by integration with MOF NPs [140]. Generally, AuNP-coated MOF NPs are synthesized mostly using three different strategies, including a one-pot approach to embed AuNPs into the cavities of MOF, post-adsorption of AuNPs onto the MOF NPs and *in situ* growth (Fig. 9) [141]. However, based on the pore size limitation of MOFs, anisotropic AuNPs can only be integrated as a core center to synthesize MOF-derived core-shell NPs. Even though many studies on the construction of core–shell AuNP-MOFs have been published, the direct construction of a well-structured core–shell based on a single anisotropic AuNPs core MOFs without further modification remains a major challenge. Because

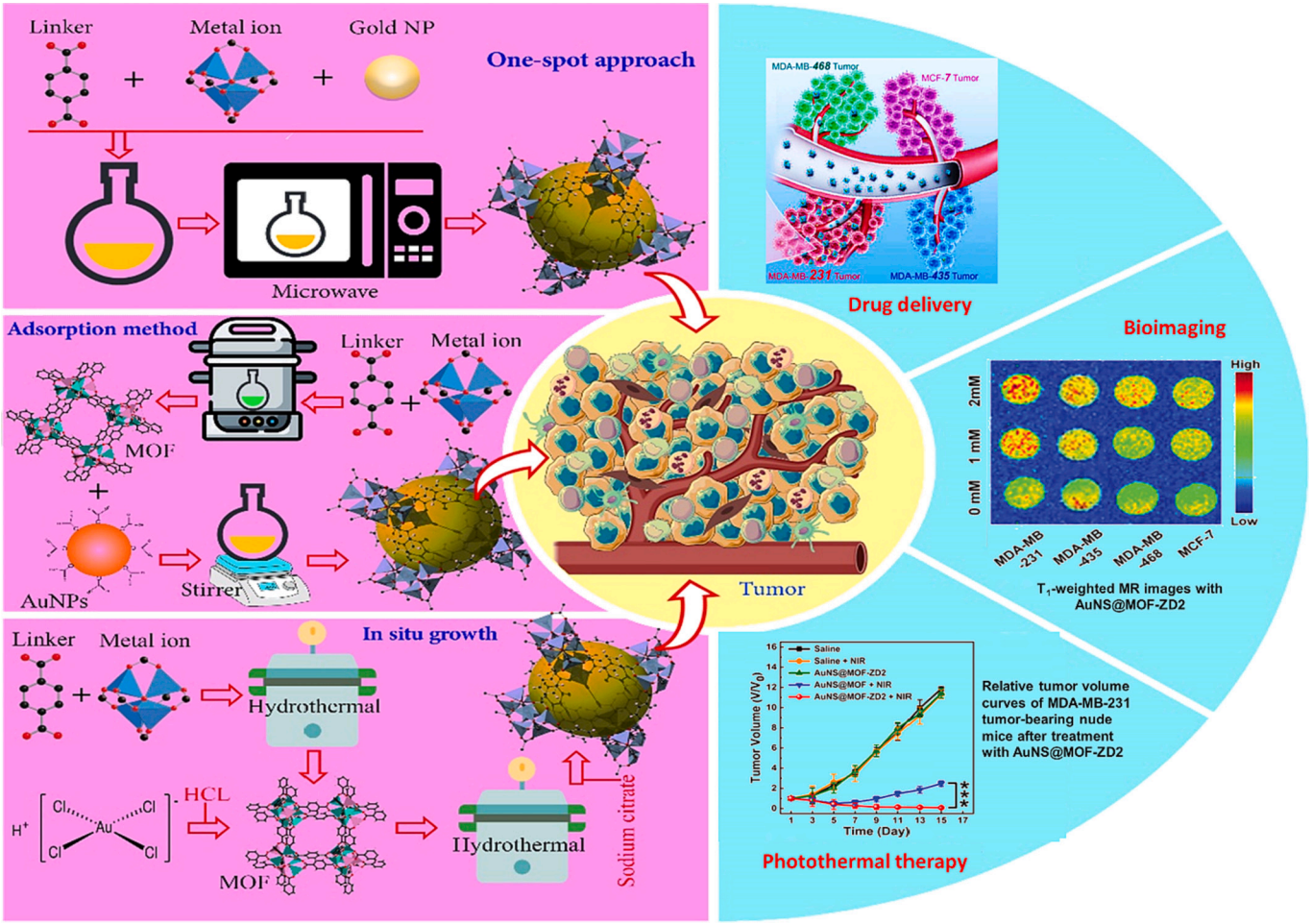

Fig. 9. The most important methods for producing AuNP@MOF NPs and a summary of their application in tumor therapy. Adapted from Ref. [144].

of their non-toxic and biodegradable properties, MIL-101-NH_2(Fe)-based NPs have been identified as excellent candidates for the development of outer shells of NP@MOF nanostructures among various types of MOFs [142,143]. Furthermore, amino groups are extremely beneficial for further functionalization in the development of TDDSs [144].

In this context, Zhang and co-workers [144] constructed a short peptide (ZD2)-modified Au nanostar (NS)@MOF core–shell nano-platform with a dimension of 225 nm through encapsulation of polymer-coated AuNS within MIL-101-NH_2(Fe) (abbreviated as AuNS@MIL-101-NH_2(Fe)-ZD2), which showed potential T_1-weighted MRI and selective PTT toward cancer cells (MDA-MB-231). To fabricate a well-structured core–shell AuNS@MOF NP, the coating approach with a step-by-step strategy (4 cycles) was performed. Finally, it was revealed that the constructed system has selective targeting capacity toward MDA-MB-231 cells , suggesting the promising utilization in visualized theranostics of breast cancers [144]. In addition to the high chemical stability determined by the zeta potential analysis, AuNS@MOF-ZD2 NPs induced high toxicity on MDA-MB-231 cells, particularly in combination with PTT, which led to a potential decrease in the breast tumor volume. Surfactants are commonly used in the fabrication of AuNPs to modify their surface [145]. However, surfactant-modified AuNPs trigger high toxicity against off-target tissues, and some approaches are required to mitigate the cytotoxicity of AuNPs and aid associated clinical translation. For example, removing surfactants from AuNPs through surface modification might be an ideal strategy enabled by ligand exchange [146] or electrostatic adsorption [147]. Chien and co-workers [148] developed a core–shell AuNP@MIL-100(Fe) nanostructures for PTT by removing the surfactants from the surface of AuNPs and using live cell-associated targeted cancer therapy. Macrophages could reach the hypoxic environment of tumor cells through penetrating blood-vessel barriers [149]. Thus, macrophage-based NP transport in the development of DDSs has recently been demonstrated as a potential strategy for tumor targeting [150,151]. Also, circulating monocytes show the potential to differentiate into macrophages, and their uptake is influenced by cytokines and chemokines [CCL2 (monocyte chemotactic protein-1, MCP-1)] [152]. Because cancer cells overexpress chemokines and cytokines, the hypoxic environment of tumors mediates the penetration of macrophages [153]. The drug delivery *via* macrophage/monocyte can then reach the deeper parts of the tumor *via* the aforementioned mechanism. The relationship between macrophage penetration and CCL2 levels has been demonstrated in several types of tumors [154–156]. Therefore, Chienand co-workers [148] developed a core–shell monocyte chemoattractant protein-1 (MCP-1)/AuNP@MIL-100(Fe) to regulate cellular uptake and cytotoxicity. TEM and FTIR results determined the successful synthesis of MCP-1/AuNP@MIL-100 (Fe) with a dimension of 50 × 12 nm, and this structure also provided good biocompatibility. Furthermore, the platform attracted macrophages as evidenced by a transwell migration assay, and the NP uptake level was increased by approximately 1.5 times after MCP-1 modification, indicating that macrophages mediate a tumor-targeting process. Additionally, the tumor growth in tumor-bearing mice that received MCP-1/GNR@MIL-100(Fe) was inhibited with successive NIR exposure (on 43 days) [148]. As a consequence, based on tumor histology, proliferation rates and bioluminescence/fluorescence-mediated imaging (Fig. 10), MCP-1/GNR@MIL-100(Fe) combined with the PTT demonstrated a promising antitumor potency.

Regarding the latter one, lanthanide (Ln)-based MOFs with luminescence characteristics similar to Ln ions have emerged as potential NPs in bioluminescence-mediated imaging [157,160]. However, the majority of the Ln-MOF NPs are excited following UV–visible ($\lambda_{ex} < 500$ nm) irradiation, precluding their biological applications [161]. Developing a system with an excitation source in the NIR region can diminish the absorption of the incident irradiation by the biological system, therefore successfully mitigating the side effects triggered by the excited irradiation. A two-photon responsive ligand can be integrated with NPs to shift their excitation from the UV–visible region to the NIR or IR regions [162]. As a result, a smart-temperature sensitive nano-platform deriving from two-photon absorption Ln-MOF can be constructed to recognize thermal biosensing in the process of PTT, which could be used for the development of an integrated system for bioimaging and treatment. For this reason, Zhang and co-workers [157] developed core–shell Ln-MOF (AuNP@Tb-MOF-[4-(2,4,6-trimethoxyphenyl)-pyridine-2,6-dicarboxylic acid (TMP-DPA) (T)]@DOX nanostructures to achieve fluorescence imaging-guided photo-stimulated combined PTT and chemotherapy and controlled drug release following NIR exposure. Thus, the improved fluorescence lifetime and sensitive transition of the Tb^{3+} endowed AuNP@Tb-MOF-T NPs the capacity for ultrasensitive temperature-biosensing. Finally, DOX was loaded into the constructed core–shell platform and activated with 808 nm laser light to achieve a potential fluorescence imaging-guided multimodal therapy [157]. This study proposed a promising strategy to create a multifunctional complex for temperature biosensing in cancer therapy. To address the requirement for UV–visible light to excite the MOFs, Zhou and co-workers [28] published an earlier report focusing on the construction of a single-crystalline mesoporous porphyrinic MOF on the surface of individual AuNRs . The core–shell AuNR@MOF showed the benefit of a mesoporous structure, and a laser-induced $^1O_2$ activation response, denoted by the porphyrinic MOF shell, as well as plasmonic photothermal

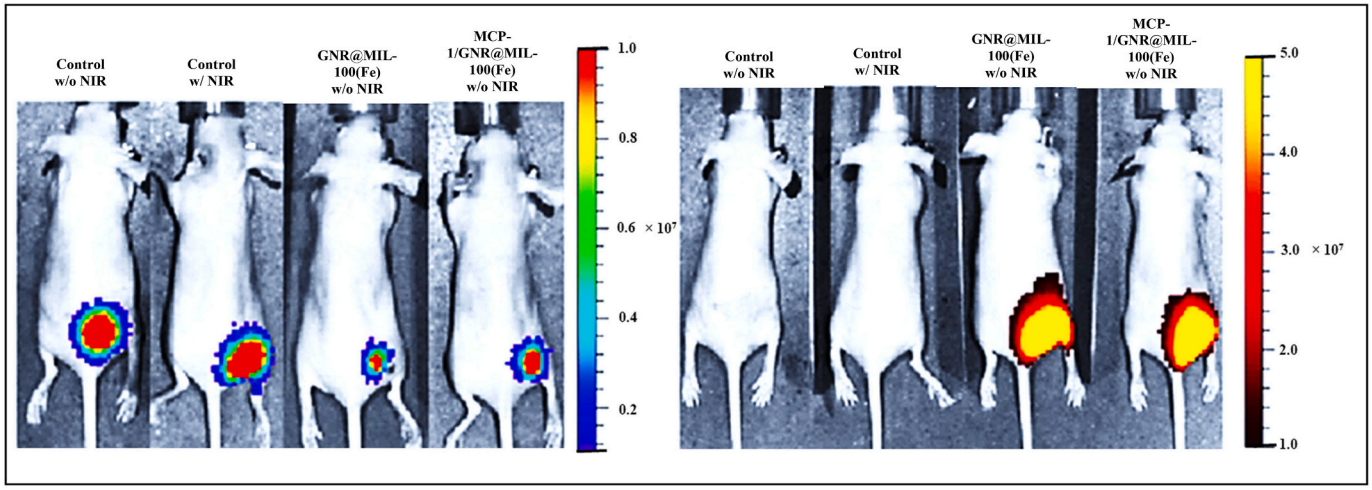

Fig. 10. PTT using monocyte chemoattractant protein-1 (MCP-1)/AuNP@MIL-100(Fe) and evaluating their antitumor efficacy via *in vivo* bioluminescene (left) and fluorescence imaging ((right) [148].

conversion, which is a feature of AuNRs, when used under a NIR laser irradiation (Fig. 11) [28]. Consequently, by combining PTT and PDT, this system can be used as an exceptional cancer treatment system. As a consequence, modifying the crystallographic orientation of NPs into core–shell structures may be a promising strategy for combinational phototherapy against tumor cells.

Furthermore, multiple NPs can be integrated into a single system using a simple and feasible approach. For example, Guo and co-workers constructed a multifunctional complex by depositing layer-by-layer MOFs *in situ* on core–shell AuNRs-mesoporous SiO_2 (MSN) NPs (fabricated *via* an oil–water biphase reaction approach), which was further modified with hyaluronic acid (HA) [158]. The developed DOX@AuNRs-MSNs-MA nano-platforms with a dimension of 160.24 nm were then found to effectively integrate targeted combined chemo-PTT and tri-modal MR-CT-PA imaging into a single system. DOX@AuNRs-MSNs-MA nanostructures also demonstrated several advantages, including increased drug loading capacity, targeted drug delivery and NIR laser-stimulated drug release. As a result of the NIR laser light, these systems showed exceptional combined efficacy for combating the 4 T1 cells *in vitro* (dose-dependent) and inhibiting breast tumor growth *in vivo* (6-fold reduction in tumor volume). The promising tri-modal *in vivo* imaging of the tumor model indicated that integrating MOF with other NPs can confer precise and well-organized theranostics.

However, two major drawbacks preclude the clinical application of core–shell MOF structures. The first point is the stability of these platforms in TME, and the second one is the requirement for high temperature of the tumor site (> 50 °C) for efficient PTT-mediated tumor ablation [163,164]. Although PTT-induced mild hyperthermia (below 50 °C) can effectively inhibit tumor growth for a longer period, cancer cells are inclined to upregulate the expression of heat shock proteins (HSPs) to protect themselves from heat-induced stress and show high resistance to PTT [165]. Recently, it has been demonstrated that combining heat shock protein inhibitors such as gambogic acid (GA) with MOFs has a highly effective inhibitory effect on the restoration of cancer cell heat sensitivity [159]. To overcome these drawbacks, Li and co-workers [159] developed a core–shell AuNS@Zr^{4+} with tetrakis (4-carboxyphenyl) porphyrin (TCPP)-GA coated with a PEGylated liposome (PL) (AZGL) with a dimension of ~190.1 nm based on a facile one-pot coordination reaction . GA and liposomes increased cancer cell sensitivity to PTT and MOF stability in TME, respectively. The *in vivo* and *in vitro* assays then indicated that photothermal [980 nm laser (0.5 W/cm^2, 10 min)] / photodynamic [660 nm laser (0.22 W/cm^2, 5 min)] synergistic therapy can effectively kill heat-resistant tumor cells in nano-platform-treated samples evidenced by different cellular/molecular assays, fluorescence and photothermal imaging, as well as assessing the tumor volume, body weight and tumor imaging (Fig. 12) [159].

6. Gadolinium@MOF nanostructures

Immunotherapy has demonstrated enormous potential in cancer treatment, allowing for long-term control of formerly untreatable and extremely aggressive cancers [166,167]. An advanced concept of immunogenic cell death (ICD) has recently emerged, which results in the production of damage-associated molecular patterns (DAMPs) to transform cancer cells into 'self-vaccines' and activate the immune system [168,169]. Nevertheless, the eventual immunogenicity is severely restrained by the simultaneous presence of phosphatidylserine (PS) on the surface of tumor cells as a potential immunosuppressive compound [170]. To counteract the immunosuppression induced by PS, ongoing approaches largely emphasize on the application of antibodies and inhibitors to either inhibit the exposure of PS on tumor cells or reduce the formation of PS receptors in immune cells [171]. However, due to the presence of formerly exposed PS [172] and expression of PS receptors at different types of immune cells with distinct signaling pathways [171], PS blockade is ineffective in tumor immunotherapy. The advancement of alternative approaches to block PS exposure mediated by, for example, transmembrane protein 16F (TMEM 16F) in a Ca^{2+} ions-dependent pathway [173] and boost the ICD immunity is then highly demanded. According to the above-mentioned story, competitive inhibition of TMEM 16F *via* the use of heavy metals with a similar radius to Ca^{2+} but a higher binding affinity can be a potential strategy to induce cancer immunotherapy by blocking the bioactivity of Ca^{2+} binding TMEM 16F. However, based on the intrinsic limited uptake of Gd^{3+}, different DDSs have been investigated to boost its cellular internalization, primarily for biomedical applications (Table 2). One possible strategy is the application of bimetallic MOF to induce dual performance for synergistic cancer therapy. Gd-MOF-5 due to the concurrent presence of Gd^{3+} and Zn^{2+}, can be used in simultaneous triggering mitochondrial dysfunction, ER stress and TMEM 16F deactivation [174]. PEGylation of Gd-MOF-5 NPs improve their pharmacodynamic properties after intravenous administration [174].

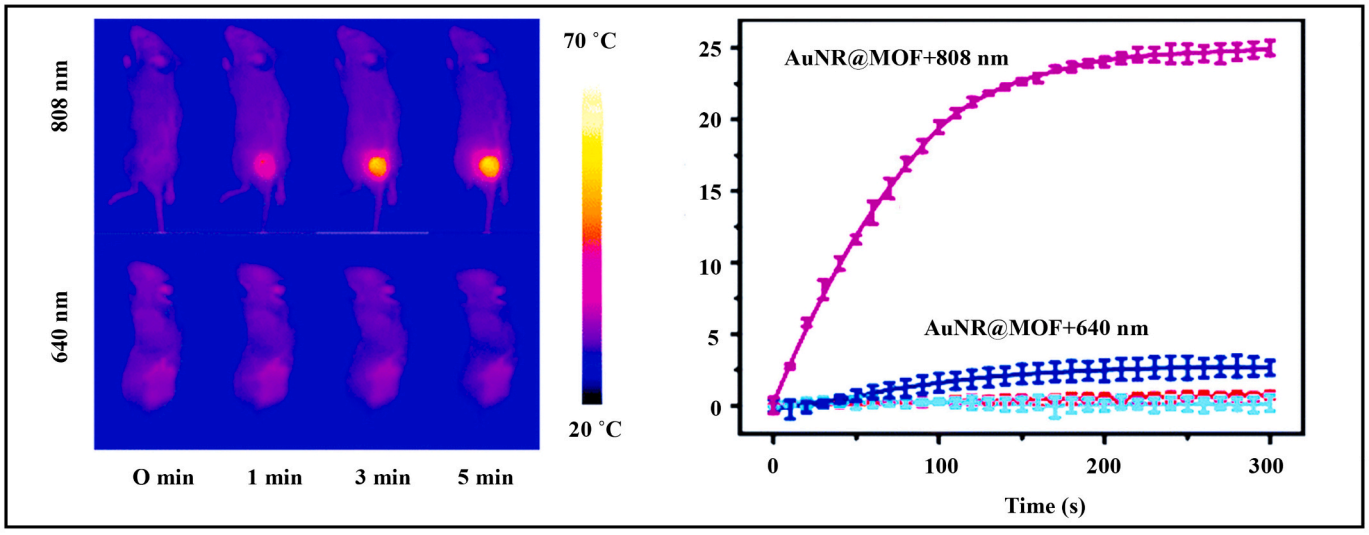

Fig. 11. Core–shell AuNR@mesoporous MOF heterostructures for combinational phototherapy of solid tumors. IR thermal images of 4 T1-tumor-bearing mice incubated with AuNR@MOFs with NIR irradiation (left), the temperature increase at the tumor site (right) [28].

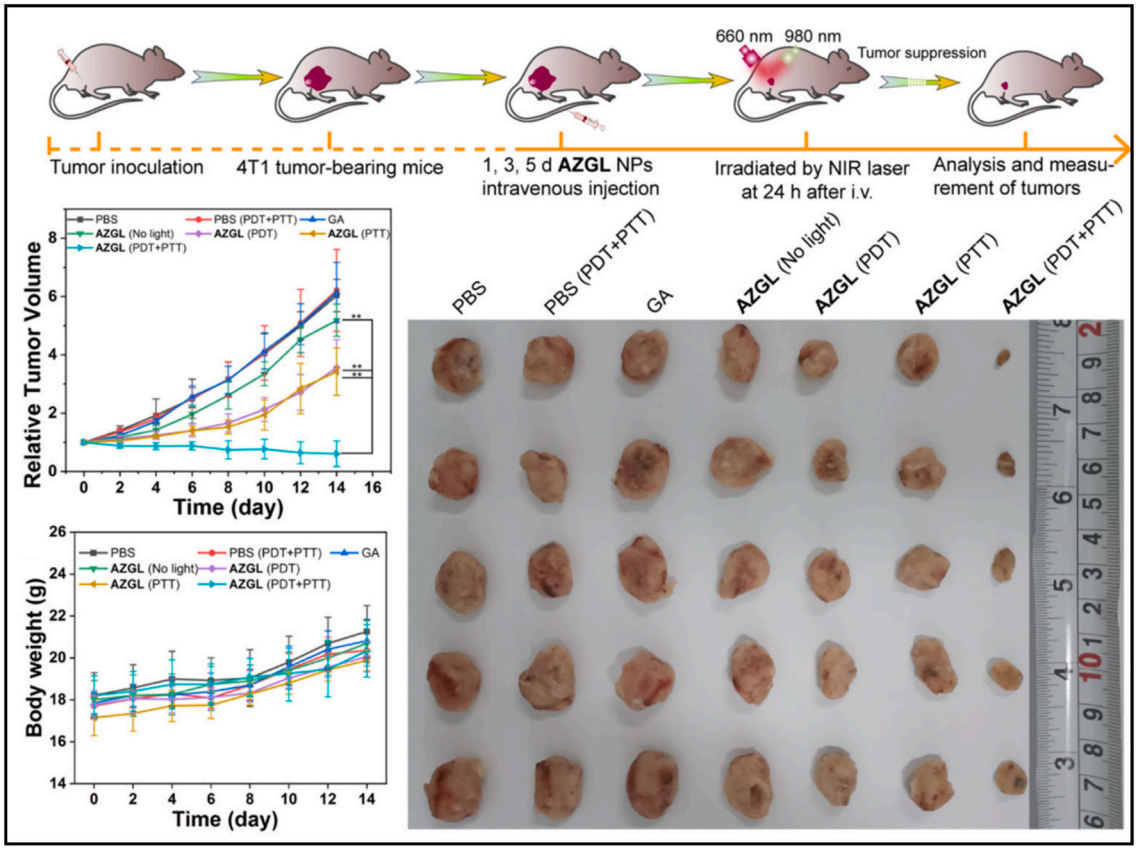

Fig. 12. Synergistic PTT-PDT-chemotherapy for breast cancer using liposome-coated core–shell AuNS@NMOF NPs modified with gambogic acid (GA), heat-shock protein-90 inhibitor, (abbreviated as AZGL). Schematic presentation of NIR light-induced combinational therapy, tumor growth curves, tumor images on the 14th day, and the body weight changes [159].

7. Other NP@MOF nanostructures

ZIF-8 contains a large number of pore cavities (11.6 Å) for potential drug loading and a small pore opening (3.4 Å) for premature drug release in off-targeted tissues [175]. Loaded cargos in pore cavities are only released in TME after NP decomposition under a mildly acidic environment.

Integrating other inorganic NPs such as mesoporous SiO_2 NPs [176] or mesoporous ZnO [177] with MOF showing high capacity in drug loading may cause the development of a new generation of pH-sensitive drug delivery platforms. However, functional groups of DOX including OH, C═O and NH_2 groups may interact weakly with Zn ions, resulting in enhanced diffusion of DOX molecules into mesoporous pores and higher drug loading in comparison with conventional mesoporous SiO_2 [177]. Additionally, the synergistic effect of the drug and Zn ions produced after the decomposition of ZnO NPs is highly effective in inhibiting cancer cell proliferation [178]. Therefore, inspired by the unique architecture of MOFs, Zheng and co-workers [177] used mesoporous ZnO NPs as drug carriers followed by their employment as the Zn precursor for the fabrication of ZnO@ZIF-8 core–shell NPs. Mesoporous ZnO NPs (core) act as not only the drug (DOX) nanocarriers but also as a source of Zn for the synthesis of ZIF-8 shell. By loading DOX in the mesoporous ZnO NP core, the ZIF-8 shell as a microporous structure (pore opening: 3.4 Å) prevented the sustained drug release at physiological pH. After interaction and cellular uptake in cancer cells, the shell architecture was decomposed at a mildly acidic environment and the loaded DOX was released from the ZnO NP core, which could also be degraded itself at an acidic microenvironment. Even though the pore volume of mesoporous ZnO NPs is generally lower than that of mesoporous SiO_2, they demonstrated greater drug-loading efficiency.

MOF-integrated NPs with reverse structures can be used as a multifunctional system for effective cancer therapy. NPs can be used as a shell for imaging, and the MOF core can be used as a platform for PPT or PDT. The main challenge in developing these platforms is the decomposition of the shell in TME. For this reason, Liu and co-workers [179] developed ZrMOF@Mn (IV) oxide (MnO_2) NPs with a fluorescence switch capability to trigger an enhanced PDT [179]. A result of the decomposition of MnO_2 NPs to Mn^{2+} ions and generation of GSH, a significant change was observed in fluorescence intensity and PDT using this platform. The GSH-sensitive activation of PDT *via* ZrMOF@MnO_2 remarkably reduced the intracellular level of GSH through a MnO_2 reduction performance, therefore stimulating an enhanced PDT efficacy. Also, the GSH-reduced Mn^{2+} ions acted as a potential system for MRI-guided tumor therapy [179]. Hence, significant changes in the cell viability of U87MG cells tumor growth and survival rate of mice with U87MG tumor were observed after treatment with ZrMOF@MnO_2 under laser irradiation [179].

Moreover, to achieve potential PDT, in addition to conversion of O_2 to $^1O_2$, sufficient oxygen supply is required to overcome tumor hypoxia environment. For this reason, some NPs with catalase-mimic activity like platinum [180], MnO_2 [181], AuNPs [182–185], and FeNPs [186] can be integrated with MOF NPs. Readers who are interested in obtaining detailed information about nanozymes could refer to some tutorial reviews [187,188].

In general, multifunctional MOF nanoprobes such as porphyrin–palladium hydride, NaLnF4@ MOF, CuS@ Fe-MOF, and Fe_3O_4@MOF could potentially apply for photoacoustic [189], luminescence [190], MRI [191], and fluorescence [94] imaging of tumor cells, respectively. Furthermore, based on the various studies published on the use of MOFs in cancer therapy, it can be concluded that core–shell MOFs can be used

to trigger anticancer effects *via* a variety of mechanisms ranging from nanocatalytic [192,193] to combined synergistic strategies [27,194].

8. Factors affecting prolonged drug delivery and cancer therapy of core–shell@MOF nanostructures

According to a survey of the results reported in several published papers, the weak stability of MOF, lack of strong dispersive interaction in biological fluids, as well as low level of drug adsorption limit the potential applications of MOF in biomedical fields. Combining inorganic NPs with MOF appears to be a promising strategy for addressing these issues. Modification of MOF with O_2-containing functional moieties derived from inorganic NPs can improve their colloidal stability and formation of some pores [195,196]. Additionally, the active sites of inorganic NPs can boost the drug adsorption capacity of modified MOFs [196]. Consequently, it can be indicated that colloidal stability and drug loading efficacy of MOF can be improved by the development of NP@MOF core–shell nanostructures. However, the physicochemical properties of core–shell MOF NPs could not endow a long residual time in the targeted site, resulting in decreased drug bioavailability. To overcome this concern, the development of biopolymer-based nanocomposites can offer significant advantages over conventional modifications for the development of drug delivery systems [197,198]. The muco-adhesive and pH-sensitive characteristics of the biopolymers could result in a longer residual time and sustained drug delivery in the tumor site [199–201]. Biopolymer-modified MOF nanostructures with distinct physicochemical properties may be useful in cancer therapy by regulating drug bioavailability and improving biosafety [202]. It is possible to tailor the physicochemical properties of biopolymer-modified nanostructures based on the type of synthesis method used [196]. For example, Pooresmaeil and co-workers developed 5-Fu-loaded Zn-MOF@GO microspheres modified with chitosan for potential drug delivery against human breast cancer cells [196]. They showed the good colloidal stability of prepared nanocomposite with a spherical shape and a size in the range of 20–40 μm. Additionally, the prepared platform displayed a high drug loading value (45%), a promising swelling degree (260.5%) in acidic pH, biocompatibility, increased cellular uptake, and tumor drug delivery capability. Furthermore, a tight interaction between some biopolymers such as chitosan and alginate can be stimulated through electrostatic interactions to provide higher mechanical stability as well as anticancer activities than unmodified MOFs [203,204]. Additionally, polymers can be used to modify the rapid clearance of MOF from the body associated with a positive charge of MOF. Polymers can be used to not only protect MOFs from degradation and reverse their positive charge, but it can also be used to improve drug loading [205]. Besides, the polymer coating can be developed to serve as a stimuli-sensitive platform in TME. For this reason, Hu and *co*-workers developed a pH-sensitive polymer (OEAM)-modified MOF nanostructure (153 $\pm$ 28 nm) with several advantages, including increasing negative charge on the surface of MOF (−33 mV) to ensure its prolonged circulation time, improving MOF cellular uptake and boosting cisplatin and DOX loading to overcome multidrug resistance [205].

Moreover, MOF nanostructures can be constructed using different metal ions, resulting in the formation of inorganic clusters during the fabrication process [208]. Also, organic linkers with various geometries (linear, triangular, or square planar) can be used in the synthesis of MOFs [209]. The size and morphology of MOF nanostructures can be associated with the ionic charge of inorganic clusters, the geometry of organic linkers and their interaction [210]. Accordingly, the interaction of MOFs with the inorganic NP surface during the synthesis of core–shell NPs may play an important role in the drug delivery properties of these NPs. The drug release behavior can display different patterns based on the unique properties of core–shell MOFs. Typically, a burst drug release pattern is followed by a sustained drug release, which reveals that core–shell formulation can manipulate drug release in comparison with a free drug [211].

In general, unique features of the TME are distinguished by hypoxia, mildly acidic and excessive H_2O_2. As a result, core–shell MOF nanostructures should be a multifunctional complex capable of performing Fenton-mimic reactions with excessive H_2O_2 in TME to overcome hypoxia while also exhibiting a pH-sensitive drug release pattern. Additionally, in order to maximize the efficacy of imaging-guided tumor treatment, a potential co-delivery platform should allow for the simultaneous loading of individual cargo at different compartments without mutual interaction. Afterward, the developed nanostructures can be further modified with targeting groups. The development of core–shell nanostructures as heterogeneous hybridization is one potential strategy for fulfilling these conditions, which can benefit from the merits of various nanocarriers and, as a result, provide the hybrid nanostructure with exceptional chemical and physical properties. For this reason, Wu and co-workers fabricated a core–shell dual MOFs (MIL-88-ICG@ZIF-8-DOX) for co-delivery of indocyanine green (ICG), a photosensitizer, and DOX. MIL-88 with enzyme-mimic activity can adjust its pore size to the geometry of the drug based on breathing behavior, whereas ZIF-8 shows a pH-sensitive degradation. Thus, the developed MIL-88-ICG@ZIF-8-DOX core–shell nanostructure can be applied for synergistic PTT/PDT/chemotherapy of tumors (Fig. 13a) [206]. Also, the silanization of MOF NPs can improve the colloidal stability of core–shell nanostructures in bio-fluids, result in potential functionalization, and inhibit the uncontrolled release of encapsulated drug [207]. The thickness of the shell can be varied by the duration of silanization which may affect the colloidal stability of the composites in a number of model physiological media, enable the grafting of target molecules to the surface, and prevent an uncontrolled release of their cargo. Core–shell UiO-66@SiO_2/F127-FA can be used as a potential candidate in targeted drug delivery for MCF-7 breast cancer cells (Fig. 13b) [207].

9. Cellular uptake, biocompatibility and biodegradability of core–shell@MOF nanostructures

MOF can serve as the shell of the nanostructure and shield the inorganic NPs as the core thanks to steric stabilization. Additionally, the shell structure may modulate the formation of protein corona, resulting in the formation of a biocompatible core–shell nanostructure. Modulation of the physicochemical characteristics of such MOF-based nanostructures can also be used to circumvent the uptake of core–shell MOF nanostructures by the reticuloendothelial systems (RES). Furthermore, modification of MOF can regulate the biocompatibility and targeting possibilities of these nanostructures, whereas the core structure can be designed to form a complex with drug compounds. This strategy could be typically used to solubilize hydrophobic drugs with a low solubility in biological fluids.

While it has been reported that free small drug compounds are taken up by cells *via* a passive mechanism, the majority of macromolecules and nanostructures pass through the bilayer *via* endocytosis. Although numerous researchers have studied the endocytosis mechanism, many aspects remain poorly uncovered *in vivo*. The exploring of the subcellular targeting is pivotal for the application of core–shell MOF nanostructures, especially for the targeted delivery of nonpolar compounds. For this reason, Chen and co-workers developed a core–shell MOF nanostructure by combining g-C3N4 as a PDT agent with a ZIF-8 shell that could also carry DOX for potent combinational cancer therapy [212]. The potency of cancer therapy can be significantly boosted by combining DOX with the PDT effect caused by g-C3N4 nanosheets. Moreover, this system might be equipped with dual-color imaging capabilities for monitoring the drug release behavior thanks to the red and blue fluorescence of DOX and g-C3N4 nanosheets, respectively. The cellular uptake of g-C3N4@ZIF-8 core–shell nanostructures was investigated using A549 cells [212]. In the control cells treated with no agent, they do not display any fluorescent signal [Fig. 14a(i)]. For the cells treated with core–shell nanostructures in the absence of DOX [Fig. 14a(ii)], the distribution of blue fluorescence in the subcellular part indicates that these NPs were

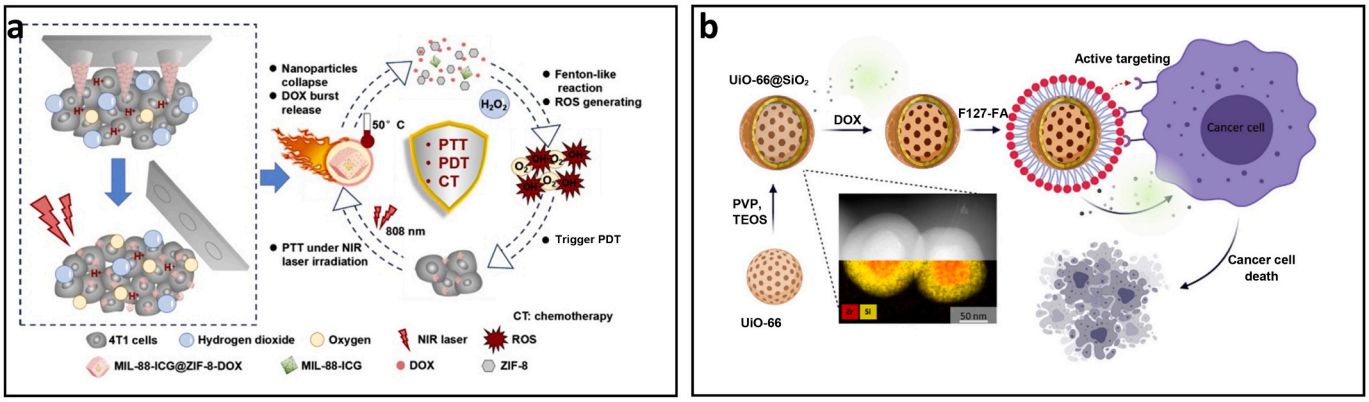

Fig. 13. (a) MIL-88-ICG@ZIF-8-DOX core-shell nanostructures for synergistic therapy of tumor [206]. (b) Development of core–shell UiO-66@SiO_2/F127-FA for targeted cancer therapy [207].

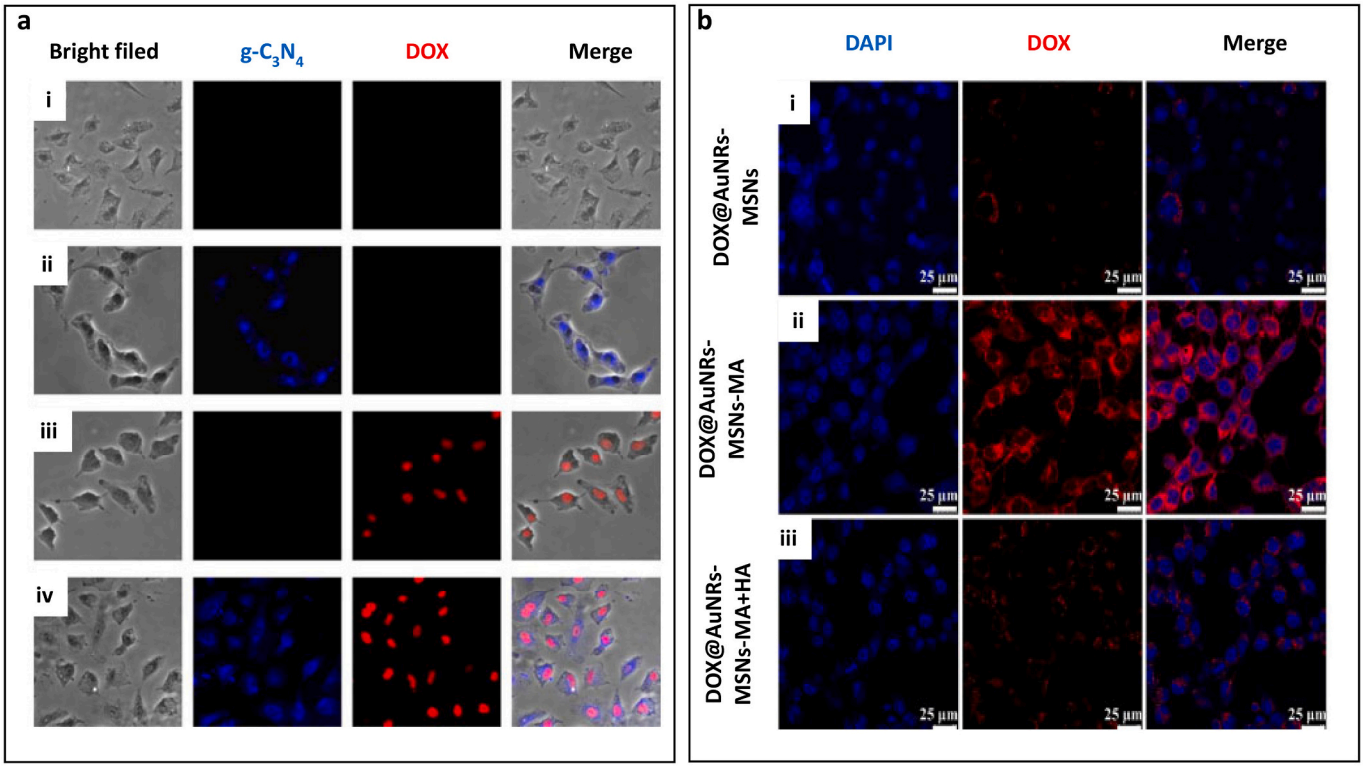

Fig. 14. (a) A549 cells incubated with no agent (i), g-C_3N_4 (ii), free DOX (iii), DOX loaded-g-C3N4@ZIF-8 core–shell NPs (iv) [212]. (b) Interaction of DOX loaded AuNR-MSN-MOF core–shell nanostructures with 4 T1 cells, unmodified sample (i), modified sample with HA (ii), pre-treatment of cells with free HA (iii) [158].

endocytosed and transported into the cytoplasm. Additionally, a free DOX compound with an intrinsic red fluorescent signal was demonstrated to transport in the nuclei [Fig. 14a(iii)]. In addition, treated A549 cells with DOX-loaded nanostructures [Fig. 14a(iv)], showed the nuclei and cytoplasm with red and blue fluorescence intensities, respectively. These findings demonstrated that the g-C3N4@ZIF-8 core–shell nanostructures loaded with DOX are capable of delivering DOX into the cell nucleus and enabling dual-color fluorescence-based imaging [212].

Also, Shang and co-workers developed fluorescent (indocyanine green)-labeled AuNR@MOF core–shell nanostructures and assessed the cellular uptake of these platforms by fluorescence microscopy of U87MG cells [213]. The results showed a significant uptake efficiency when cells were treated with AuNR@MIL-88(Fe) core–shell nanostructures for 1 h. However, the authors did not explore the detection of fluorescence signals in cellular organelles or the nucleus. Besides, Ren and co-workers using confocal laser scanning microscopy displayed that cellular internalization of DOX-loaded ZIF-67 encapsulated with a layer of ZIF-8 loaded with PS (ZDZP NPs) was associated with endocytosis based on a time-dependent manner in 4 T1 cells and potential accumulation of DOX inside the nucleus [214].

Also, to maximize the therapeutic potency of a single nanostructure, a multifunctional nanostructure with coordinated interactions should be developed to potentially stimulate targeted combination therapy-guided multi-modal imaging of tumors. For this reason, Guo and co-workers developed core–shell AuNR-MSNs covered by a layer of MOF shell to achieve chemo-PTT combination therapy we well as tri-modal imaging [158]. Moreover, the developed system was modified by HA for potential targeted capability. Confocal microscopy study showed that DOX@AuNRs-MSNs treated 4 T1 cells [Fig. 14b(i)] exhibit significantly

lower levels of red fluorescence signal than do cells with functionalized nanostructures [Fig. 14b(ii)] [158], indicating that the endocytosis potency of the functionalized platform is much better than the unmodified samples. Additionally, to assess the receptor-mediated endocytosis by developing multifunctional complex, free HA as a typical blocker of the receptors was used. As exhibited in Fig. 14b(iii), once the cells were pre-incubated with HA, the intracellular red fluorescence signal was significantly quenched, which revealed that the intracellular delivery of DOX-loaded AuNRs-MSNs-MA is blocked [158].

For that reason, it can be claimed that changing the physicochemical properties (morphology, size, surface charge, surface hydrophilicity, and hydrophobicity) and modification of core–shell MOF nanostructures by targeting moieties can maximize their possible interaction with cells. Each of these parameters creates different reactions at the cellular level according to the nature of the inorganic NPs (core) and MOFs used and the type of cells. These interactions and subsequent endocytosis can stimulate a wide range of reactions at the subcellular level, including significant damage to the membrane, mitochondria, nucleus, lysosome, and DNA, which ultimately changes the nature of the cell and causes targeted cell death.

Regarding the biocompatibility and biodegradability of MOFs for biomedical implementations, it should be emphasized that several physicochemical properties could modulate the biocompatibility and biodegradability features of MOFs such as the type of the metal ions as well as organic linkers, dimension, surface chemistry, and colloidal biostability. Manipulation of The biodistribution of MOFs *in vivo* can lead to modulation of their pharmacokinetics, toxicity and associated immune response. By conducting such investigations, we can develop future biocompatible platforms that may be able to safely be translated into the pharmaceutical consumer market in the near future. For further information regarding the biocompatibility and biodegradability of MOFs, the readers refer to [215].

10. Enhanced permeation and retention (EPR) effect of core–shell@MOF nanostructures

Exploring tumor-selective drug delivery and boosted endocytosis using core–shell MOF nanostructures can provide useful information about the development of effective cancer therapeutics. Although, the active delivery mechanism can be upregulated *via* the modification of MOF nanostructures with targeting moieties, including oligosaccharides, Apts, or antibodies, passive targeting into permeable tumor tissue is also quite significant [215]. The development of NP-based drug delivery platforms has been supported by recent reports regarding the enhanced permeability and retention (EPR) effect of tumor vascular and their corresponding targeting in tumor sites [4]. In other words, the EPR effect derived from the unique physiological properties of solid tumors (permeable feature of blood vessels and lack of lymphatic drainage system) is a mechanism by which nanostructures accumulate in solid tumors [4]. When the dimension of nanostructures is in the range of 20–150 nm, the EPR-mediated uptake of MOFs by tumor cells increases [216]. However, scaling down of the NPs remains a remarkable concern for MOF-mediated imaging of tumor tissue. Thus, fabrication of potential MOF nanostructures with an optimum size to achieve both potential imaging and EPR effect is challenging. For this reason, Shang and co-workers fabricated the Au@MIL-88 core–shell nanostructure with a size of about 89 nm to achieve promising triple-modality imaging of the U87 tumor as well as high passive uptake by tumor cells as a consequence of the EPR effect [213].

Therefore, it seems that core–shell MOF nanostructures can be used as interesting nanocarriers to stimulate EPR effects due to their specific interaction with tumor cells, good biocompatibility and hydrophilicity, multiple synthetic methods, and cost-effective [217,218]. Based on the unique characteristics of TME, one of the key concerns that should be addressed regarding the NP-based DDS is the development of intrinsic or extrinsic stimuli-responsive smart platforms. For example, Wang and co-workers developed a $Mn_3[Co(CN)_6]_2$@MIL-100(Fe) core–shell nanostructure for targeted co-delivery of Fe(III) and AS mediated by EPR effect in a pH-sensitive drug release manner under multimodality imaging [111]. In comparison with free drugs, the encapsulated drug represents remarkably increased targeted tumor delivery by EPR effect with minor toxicity. *In vivo* assays indicated that the anticancer potency of drug-loaded $Mn_3[Co(CN)_6]_2$@MIL-100(Fe) core–shell nanostructure was about 5 folds greater than that of its free counterpart, making it a potential EPR-associated DDSs. Additionally, based on the EPR effect as well as promising MR imaging capabilities, Fe_3O_4@UiO-66 core–shell nanostructures have been reported as a possible candidate in DOX delivery to HeLa tumor *in vivo* [214]. Camptothecin-loaded AuNR@MOF core–shell nanostructures can accumulate in solid tumors through the EPR effect, leading to an improved cancer therapy mediated by NIR light-triggered drug release, which is about the extrinsic-sensitive DDSs [219].

To develop a stimuli-responsive DDS following the EPR effect, anticancer agents can be loaded into pH-sensitive MOF nanostructures (shell) or attached to inorganic NPs (core) by specific linkers such as acid-labile or peptide spacers that are sensitive to pH or temperature. In addition, the inorganic NPs can be used as nanozymes to mimic the catalase-like or peroxidase-like activity to overcome the hypoxia and low levels of ROS in TME, respectively [217,220,221]. Also, the EPR effect can be combined with active targeting enabled by core–shell MOF nanostructure to maximize the cancer therapeutics [222].

However, it should be highlighted that many active or passive targeted DDSs work effectively under laboratory circumstances despite the probability that, when applied *in vivo*, they may not promote drug accumulation in solid tumors. These concerns may be caused by the low density of receptors on the surface of tumor cells, steric hindrance of receptors, low colloidal stability of carriers, and their interaction with RES. Additionally, the degree of angiogenesis, tumor growth and intratumoral pressure play a key role in the EPR effect-mediated cancer therapeutics enabled by nanostructures.

11. Challenges and future perspectives

Although MOFs have been extensively studied as drug nanocarriers, they have several drawbacks, including cytotoxicity, low stability and biodegradability and complex and multistep fabrication processes that vary between MOF species. Therefore, the integration of MOFs with other NPs especially inorganic counterparts was studied as a promising way to develop a new class of porous core–shell nanostructures with potential characteristics. However, inorganic NPs are prone to self-aggregation in bio-fluids in the presence of intrinsic and extrinsic factors. Also, the stability of core–shell MOF in bio-fluids heavily depends on the interaction between functional groups of inorganic NPs and metal centers in the MOF nanostructure governed by coordination chemistry.

Different studies have reported the co-delivery of chemotherapeutics enabled by core–shell MOFs, however, the main challenge for these types of DDSs is the contradictive requirement between blood circulation and tumor targeting. Positive and negative NPs show rapid clearance and low rate of endocytosis, respectively. Thus the advancement of smart core–shell MOF nanostructures to overcome these challenges and promote drug delivery is greatly appreciated.

Multi-drug resistance solid tumors have become a major impediment in the inhibition of malignant tumors. In light of the treatment of this type of cancer, a potential and smart core–shell MOF nanostructure with different drugs encapsulated in individual structures to conduct synergistic cancer therapy should be developed to overcome this major challenge in the treatment of malignant cancers.

Although the core–shell MOF-based DDSs have boosted the drug loading and targeting potency to some extent due to porous structure and EPR effects, respectively, they still have some defects, such as lack of potential targeting, reduced level of endocytosis and low cellular uptake. So, to address these concerns, a large number of functional

targeting core–shell MOF nanostructures have been developed. However, some ligands, such as FA, can stimulate cancer cell growth and differentiation, resulting in a decrease in therapeutic efficacy. Accordingly , selecting an appropriate core–shell MOF nanostructure capable of both receptor targeting using multi-target antagonists and stimulating apoptosis in tumor cells is critical. Moreover, the targeting group should have a coordinated site to show potential affinities with the metal active site of MOF, which is an ideal folate modifying group.

Inorganic NPs, MOFs and their combinations have also shown enzyme-like activities, which can be used to overcome low levels of O_2 and free radicals in tumor cells. It should be noted, however, that the nanozyme activity of NPs is heavily influenced by unwanted interactions with bio-fluids and the formation of the protein corona. For that reason, some strategies for manipulating the formation of protein corona on the surface of core–shell MOF nanostructures should be considered.

Additionally, to enhance the efficacy of cancer theranostics using core–shell MOF nanostructures, several parameters, such as temperature, time, concentration, and pH should be adjusted.

12. Conclusion

In conclusion, we surveyed several novel core–shell MOF nanostructures fabricated from inorganic NPs as core and different MOF nanostructures as shell to potentially benefit from the targeted drug delivery, *in vivo* multi-mode imaging and combined tumor therapy. Detailed overviews on the fabrication of MOFs indicated that the nucleation mechanism initiates the growth of MOFs on inorganic NPs. Due to their capacity to load a high concentration of drugs and release them over a sustained period in a stimuli-responsive manner, core–shell MOF nanostructures are known as exceptional drug carriers. Core–shell MOF nanostructures can be used in the development of potential endogenous or/and exogenous stimuli-responsive DDS. Also, with the high loading efficacy of chemotherapeutics, inherent magnificent photothermal and photodynamic conversion features and multimodal imaging, the core–shell MOFs could stimulate multimodal imaging-guided combination cancer therapy. As a result of the heterogeneous hybridization of two NPs with different biochemical functions, core–shell MOF nanostructures represent promising theranosticsystems.

Funding

This project was partly funded by Henan Province International Science and Technology Cooperation Project, (NO: 232102520025) (S. K), 2021 Young and Middle-Aged Academic Leaders of Health in Henan Province, (NO: HNSWJW-2021001), and Program for Science &Technology Innovation Talents in Universities of Henan Province, (NO: 22HASTIT047).

Author contribution

Suliman Khan, William C. Cho, Yasaman Vahdani, Rabeea Siddique, Majid Sharifi, Laila Abdulmohsen Jaragh-Alhadad, Setareh Haghighat, Xiaoju Zhang: Conceptualization, Literature survey, Writing, Editing, Figure preperation/adaptation/reprinting; **Mojtaba Falahati, Timo L.M.ten Hagen, Qian Bai:** Conceptualization, Supervision, Writing, Editing.

Declaration of Competing Interest

The authors declare no conflict of interest.

Data availability

No data was used for this review article. This paper presents some figures that most of them do not belong to the authors; they have been reprinted/adapted from the cited references.

Acknowledgements

We appreciate the Editors and Reviewers of Advances in Colloid and Interface Science for constrictive comments that have increased the scientific integrity of this review paper.

References

[1] van den Boogaard WM, Komninos DS, Vermeij WP. Chemotherapy side-effects: not all DNA damage is equal. Cancers. 2022;14:627.
[2] Mitchell MJ, Billingsley MM, Haley RM, Wechsler ME, Peppas NA, Langer R. Engineering precision nanoparticles for drug delivery. Nat Rev Drug Discov 2021; 20:101–24.
[3] Seynhaeve A, Amin M, Haemmerich D, Van Rhoon G, Ten Hagen T. Hyperthermia and smart drug delivery systems for solid tumor therapy. Adv Drug Deliv Rev 2020;163:125–44.
[4] Sharifi M, Cho WC, Ansariesfahani A, Tarharoudi R, Malekisarvar H, Sari S, et al. An updated review on EPR-based solid tumor targeting nanocarriers for cancer treatment. Cancers. 2022;14:2868.
[5] Palazzolo S, Bayda S, Hadla M, Caligiuri I, Corona G, Toffoli G, et al. The clinical translation of organic nanomaterials for cancer therapy: a focus on polymeric nanoparticles, micelles, liposomes and exosomes. Curr Med Chem 2018;25: 4224–68.
[6] Zheng Y, Hasan A, Babadaei MMN, Behzadi E, Nouri M, Sharifi M, et al. Exosomes: multiple-targeted multifunctional biological nanoparticles in the diagnosis, drug delivery, and imaging of cancer cells. Biomed Pharmacother 2020;129:110442.
[7] Mohamed Isa ED, Ahmad H, Abdul Rahman MB, Gill MR. Progress in mesoporous silica nanoparticles as drug delivery agents for cancer treatment. Pharmaceutics. 2021;13:152.
[8] Sharifi M, Hosseinali SH, Yousefvand P, Salihi A, Shekha MS, Aziz FM, et al. Gold nanozyme: biosensing and therapeutic activities. Mater Sci Eng C 2020;108: 110422.
[9] Nie Z, Vahdani Y, Cho WC, Bloukh SH, Edis Z, Haghighat S, et al. 5-fluorouracil-containing inorganc iron oxide/platinum nanozymes with bimodel drug delivery and peroxidase-like activity for the treatment of breast cancer. Arab J Chem 2022;103966.
[10] Khan S, Sharifi M, Hasan A, Attar F, Edis Z, Bai Q, et al. Magnetic nanocatalysts as multifunctional platforms in cancer therapy through the synthesis of anticancer drugs and facilitated Fenton reaction. J Adv Res 2021;30:171.
[11] Lekha DC, Shanmugam R, Madhuri K, Dwarampudi LP, Bhaskaran M, Kongara D, et al. Review on silver nanoparticle synthesis method, antibacterial activity, drug delivery vehicles, and toxicity pathways: recent advances and future aspects. J Nanomater 2021;2021.
[12] Anjum S, Hashim M, Malik SA, Khan M, Lorenzo JM, Abbasi BH, et al. Recent advances in zinc oxide nanoparticles (Zno nps) for cancer diagnosis, target drug delivery, and treatment. Cancers. 2021;13:4570.
[13] Jain NS, Somanna P, Patil AB. Application of quantum dots in drug delivery. Nanosci Nanotechnol Asia 2022;12:16–31.
[14] Paul W, Sharma CP. Inorganic nanoparticles for targeted drug delivery. Biointegr Med Implant Mater 2020:333–73.
[15] Verma J, Lal S, Van Noorden CJ. Inorganic nanoparticles for the theranostics of cancer. Eur J Nanomed 2015;7:271–87.
[16] Hoskins BF, Robson R. Infinite polymeric frameworks consisting of three dimensionally linked rod-like segments. J Am Chem Soc 1989;111:5962–4.
[17] Cao J, Li X, Tian H. Metal-organic framework (MOF)-based drug delivery. Curr Med Chem 2020;27:5949–69.
[18] Mallakpour S, Nikkhoo E, Hussain CM. Application of MOF materials as drug delivery systems for cancer therapy and dermal treatment. Coord Chem Rev 2022;451:214262.
[19] Horcajada P, Serre C, Vallet-Regí M, Sebban M, Taulelle F, Férey G. Metal–organic frameworks as efficient materials for drug delivery. Angew Chem 2006;118:6120–4.
[20] Babarao R, Jiang J. Unraveling the energetics and dynamics of ibuprofen in mesoporous metal– organic frameworks. J Phys Chem C 2009;113:18287–91.
[21] Bieniek A, Terzyk AP, Wiśniewski M, Roszek K, Kowalczyk P, Sarkisov L, et al. MOF materials as therapeutic agents, drug carriers, imaging agents and biosensors in cancer biomedicine: recent advances and perspectives. Prog Mater Sci 2021;117:100743.
[22] Wu MX, Yang YW. Metal–organic framework (MOF)-based drug/cargo delivery and cancer therapy. Adv Mater 2017;29:1606134.
[23] Cai W, Wang J, Chu C, Chen W, Wu C, Liu G. Metal–organic framework-based stimuli-responsive systems for drug delivery. Adv Sci 2019;6:1801526.
[24] Gao X, Hai X, Baigude H, Guan W, Liu Z. Fabrication of functional hollow microspheres constructed from MOF shells: promising drug delivery systems with high loading capacity and targeted transport. Sci Rep 2016;6:1–10.
[25] Chen X, Tong R, Shi Z, Yang B, Liu H, Ding S, et al. MOF nanoparticles with encapsulated autophagy inhibitor in controlled drug delivery system for antitumor. ACS Appl Mater Interfaces 2018;10:2328–37.
[26] Bao Z, Li K, Hou P, Xiao R, Yuan Y, Sun Z. Nanoscale metal–organic framework composites for phototherapy and synergistic therapy of cancer. Mater Chem Front 2021;5:1632–54.

[27] Geng P, Yu N, Macharia DK, Meng R, Qiu P, Tao C, et al. MOF-derived CuS@ Cu-MOF nanocomposites for synergistic photothermal-chemodynamic-chemo therapy. Chem Eng J 2022;441:135964.
[28] Zhou Z, Zhao J, Di Z, Liu B, Li Z, Wu X, et al. Core–shell gold nanorod@ mesoporous-MOF heterostructures for combinational phototherapy. Nanoscale. 2021;13:131–7.
[29] Cai X, Deng X, Xie Z, Shi Y, Pang M, Lin J. Controllable synthesis of highly monodispersed nanoscale Fe-soc-MOF and the construction of Fe-soc-MOF@ polypyrrole core-shell nanohybrids for cancer therapy. Chem Eng J 2019;358: 369–78.
[30] Wang D, Zhou J, Chen R, Shi R, Xia G, Zhou S, et al. Magnetically guided delivery of DHA and Fe ions for enhanced cancer therapy based on pH-responsive degradation of DHA-loaded Fe3O4@ C@ MIL-100 (Fe) nanoparticles. Biomaterials. 2016;107:88–101.
[31] Cai M, Chen G, Qin L, Qu C, Dong X, Ni J, et al. Metal organic frameworks as drug targeting delivery vehicles in the treatment of cancer. Pharmaceutics. 2020;12: 232.
[32] He L, Liu Y, Lau J, Fan W, Li Q, Zhang C, et al. Recent progress in nanoscale metal-organic frameworks for drug release and cancer therapy. Nanomedicine. 2019;14:1343–65.
[33] Falsafi M, Saljooghi AS, Abnous K, Taghdisi SM, Ramezani M, Alibolandi M. Smart metal organic frameworks: focus on cancer treatment. Biomater Sci 2021;9: 1503–29.
[34] Lan G, Ni K, Lin W. Nanoscale metal–organic frameworks for phototherapy of cancer. Coord Chem Rev 2019;379:65–81.
[35] Saeb MR, Rabiee N, Mozafari M, Verpoort F, Voskressensky LG, Luque R. Metal–organic frameworks (MOFs) for cancer therapy. Materials. 2021;14:7277.
[36] Zeng JY, Wang XS, Song WF, Cheng H, Zhang XZ. Metal-organic framework mediated multifunctional nanoplatforms for cancer therapy. Adv Ther 2019;2: 1800100.
[37] Zheng Y, Zhang X, Su Z. Design of metal–organic framework composites in anti-cancer therapies. Nanoscale. 2021;13:12102–18.
[38] Osterrieth JW, Fairen-Jimenez D. Metal–organic framework composites for theragnostics and drug delivery applications. Biotechnol J 2021;16:2000005.
[39] Yang J, Yang YW. Metal-organic framework-based cancer theranostic nanoplatforms. View. 2020;1:e20.
[40] Zhou J, Tian G, Zeng L, Song X, Xw Bian. Nanoscaled metal-organic frameworks for biosensing, imaging, and cancer therapy. Adv Healthc Mater 2018;7:1800022.
[41] Yang Y, Zeng Z, Almatrafi E, Huang D, Zhang C, Xiong W, et al. Core-shell structured nanoparticles for photodynamic therapy-based cancer treatment and related imaging. Coord Chem Rev 2022;458:214427.
[42] Yaghi OM, Li G, Li H. Selective binding and removal of guests in a microporous metal–organic framework. Nature. 1995;378:703–6.
[43] Kondo M, Yoshitomi T, Matsuzaka H, Kitagawa S, Seki K. Three-dimensional framework with channeling cavities for small molecules: {[M2(4, 4′-bpy)3(NO3) 4]·xH2O}n (M = Co, Ni, Zn). Angew Chem Int Ed Engl 1997;36:1725–7.
[44] Moreno JM, Velty A, Díaz U, Corma A. Synthesis of 2D and 3D MOFs with tuneable Lewis acidity from preformed 1D hybrid sub-domains. Chem Sci 2019; 10:2053–66.
[45] Gao Z, Liang L, Zhang X, Xu P, Sun J. Facile one-pot synthesis of Zn/Mg-MOF-74 with unsaturated coordination metal centers for efficient CO2 adsorption and conversion to cyclic carbonates. ACS Appl Mater Interfaces 2021;13:61334–45.
[46] Hu Y, Zhang J, Huo H, Wang Z, Xu X, Yang Y, et al. One-pot synthesis of bimetallic metal–organic frameworks (MOFs) as acid–base bifunctional catalysts for tandem reaction. Cat Sci Technol 2020;10:315–22.
[47] Yuan S, Qin J-S, Su J, Li B, Li J, Chen W, et al. Sequential transformation of zirconium(IV)-MOFs into heterobimetallic MOFs bearing magnetic anisotropic cobalt(II) centers. Angew Chem Int Ed 2018;57:12578–83.
[48] Liu Q, Cong H, Deng H. Deciphering the spatial arrangement of metals and correlation to reactivity in multivariate metal–organic frameworks. J Am Chem Soc 2016;138:13822–5.
[49] Jiang X, Fan R, Zhang J, Fang X, Sun T, Zhu K, et al. Sequentially epitaxial growth multi-guest encapsulation strategy in MOF-on-MOF platform: biogenic amine detection and systematic white light adjustment. Chem Eng J 2022;436:135236.
[50] Koh K, Wong-Foy AG, Matzger AJ. MOF@MOF: microporous core–shell architectures. Chem Commun 2009:6162–4.
[51] Sun C, Skorupskii G, Dou J-H, Wright AM, Dincă M. Reversible metalation and catalysis with a scorpionate-like metallo-ligand in a metal–organic framework. J Am Chem Soc 2018;140:17394–8.
[52] Shultz AM, Sarjeant AA, Farha OK, Hupp JT, Nguyen ST. Post-synthesis modification of a metal–organic framework to form metallosalen-containing MOF materials. J Am Chem Soc 2011;133:13252–5.
[53] Hosseini SM, Dehghan H, Safarifard V. Enhancement of photocatalytic aerobic oxidation of benzyl alcohol with the incorporation of cobalt in Zn-based MOF via post-synthetic metal exchange. Polyhedron. 2022;212:115581.
[54] Peedikakkal AMP, Aljundi IH. Upgrading the hydrogen storage of MOF-5 by post-synthetic exchange with divalent metal ions. Appl Sci 2021;11:11687.
[55] Kassie AA, Duan P, McClure ET, Schmidt-Rohr K, Woodward PM, Wade CR. Postsynthetic metal exchange in a metal–organic framework assembled from Co (III) diphosphine pincer complexes. Inorg Chem 2019;58:3227–36.
[56] Zhou T, Du Y, Borgna A, Hong J, Wang Y, Han J, et al. Post-synthesis modification of a metal–organic framework to construct a bifunctional photocatalyst for hydrogen production. Energ Environ Sci 2013;6:3229–34.
[57] Binaeian E, Li Y, Tayebi H-A, Yuan D. Enhancing toxic gas uptake performance of Zr-based MOF through uncoordinated carboxylate and copper insertion; ammonia adsorption. J Hazard Mater 2021;416:125933.
[58] Binaeian E, Li Y, Yuan D. Improving ammonia uptake performance of zirconium-based metal-organic frameworks through open metal site insertion strategy. Chem Eng J 2021;421:129655.
[59] Liu D, Lu K, Poon C, Lin W. Metal–organic frameworks as sensory materials and imaging agents. Inorg Chem 2014;53:1916–24.
[60] Liu Y, Zhang C, Xu C, Lin C, Sun K, Wang J, et al. Controlled synthesis of up-conversion luminescent Gd/Tm-MOFs for pH-responsive drug delivery and UCL/ MRI dual-modal imaging. Dalton Trans 2018;47:11253–63.
[61] Liu Y, Jiang T, Liu Z. Metal-organic frameworks for bioimaging: strategies and challenges. Nanotheranostics. 2022;6:143.
[62] Taylor-Pashow KML, Della Rocca J, Xie Z, Tran S, Lin W. Postsynthetic modifications of iron-carboxylate nanoscale metal−organic frameworks for imaging and drug delivery. J Am Chem Soc 2009;131:14261–3.
[63] Chowdhuri AR, Bhattacharya D, Sahu SK. Magnetic nanoscale metal organic frameworks for potential targeted anticancer drug delivery, imaging and as an MRI contrast agent. Dalton Trans 2016;45:2963–73.
[64] Zhao H-X, Zou Q, Sun S-K, Yu C, Zhang X, Li R-J, et al. Theranostic metal–organic framework core–shell composites for magnetic resonance imaging and drug delivery. Chem Sci 2016;7:5294–301.
[65] Zhang Y, Wang L, Liu L, Lin L, Liu F, Xie Z, et al. Engineering metal–organic frameworks for photoacoustic imaging-guided chemo-/photothermal combinational tumor therapy. ACS Appl Mater Interfaces 2018;10:41035–45.
[66] Zhang H, Li Q, Liu R, Zhang X, Li Z, Luan Y. A versatile prodrug strategy to in situ encapsulate drugs in MOF nanocarriers: a case of cytarabine-IR820 prodrug encapsulated ZIF-8 toward chemo-photothermal therapy. Adv Funct Mater 2018; 28:1802830.
[67] Rengaraj A, Puthiaraj P, Heo N-S, Lee H, Hwang SK, Kwon S, et al. Porous NH2-MIL-125 as an efficient nano-platform for drug delivery, imaging, and ROS therapy utilized low-intensity visible light exposure system. Colloids Surf B Biointerfaces 2017;160:1–10.
[68] Cai X, Liu B, Pang M, Lin J. Interfacially synthesized Fe-soc-MOF nanoparticles combined with ICG for photothermal/photodynamic therapy. DTr. 2018;47: 16329–36.
[69] Li B, Wang X, Chen L, Zhou Y, Dang W, Chang J, et al. Ultrathin Cu-TCPP MOF nanosheets: a new theragnostic nanoplatform with magnetic resonance/near-infrared thermal imaging for synergistic phototherapy of cancers. Theranostics. 2018;8:4086–96.
[70] Jia Q, Li Z, Guo C, Huang X, Song Y, Zhou N, et al. A γ-cyclodextrin-based metal–organic framework embedded with graphene quantum dots and modified with PEGMA via SI-ATRP for anticancer drug delivery and therapy. Nanoscale. 2019;11:20956–67.
[71] Tian Z, Yao X, Ma K, Niu X, Grothe J, Xu Q, et al. Metal–organic framework/ graphene quantum dot nanoparticles used for synergistic chemo-and photothermal therapy. ACS Omega 2017;2:1249–58.
[72] Liu J, Liu T, Du P, Zhang L, Lei J. Metal–organic framework (MOF) hybrid as a tandem catalyst for enhanced therapy against hypoxic tumor cells. Angew Chem 2019;131:7890–4.
[73] Ding Y, Xu H, Xu C, Tong Z, Zhang S, Bai Y, et al. A nanomedicine fabricated from gold nanoparticles-decorated metal–organic framework for cascade chemo/ chemodynamic cancer therapy. Adv Sci 2020;7:2001060.
[74] Ma X, Ren X, Guo X, Fu C, Wu Q, Tan L, et al. Multifunctional iron-based metal–organic framework as biodegradable nanozyme for microwave enhancing dynamic therapy. Biomaterials. 2019;214:119223.
[75] Deng X, Liang S, Cai X, Huang S, Cheng Z, Shi Y, et al. Yolk–shell structured Au nanostar@ metal–organic framework for synergistic chemo-photothermal therapy in the second near-infrared window. Nano Lett 2019;19:6772–80.
[76] Rowe MD, Thamm DH, Kraft SL, Boyes SG. Polymer-modified gadolinium metal-organic framework nanoparticles used as multifunctional nanomedicines for the targeted imaging and treatment of cancer. Biomacromolecules. 2009;10:983–93.
[77] Liu J, Yang L, Cao X, Chen M, Li J, Wang X, et al. PEGylated Mn containing MOF nanoparticles for potential immunotherapy of pancreatic cancer via manganese induced activation of anti-tumor immunity. Colloid Interface Sci Commun 2021; 42:100409.
[78] Liu X, Liang T, Zhang R, Ding Q, Wu S, Li C, et al. Iron-based metal–organic frameworks in drug delivery and biomedicine. ACS Appl Mater Interfaces 2021; 13:9643–55.
[79] Zheng R, Guo J, Cai X, Bin L, Lu C, Singh A, et al. Manganese complexes and manganese-based metal-organic frameworks as contrast agents in MRI and chemotherapeutics agents: applications and prospects. Colloids Surf B Biointerfaces 2022;112432.
[80] Chen C, Ge J, Gao Y, Chen L, Cui J, Zeng J, et al. Ultrasmall superparamagnetic iron oxide nanoparticles: a next generation contrast agent for magnetic resonance imaging. Wiley Interdiscip Rev Nanomed Nanobiotechnol 2022;14:e1740.
[81] Soetaert F, Korangath P, Serantes D, Fiering S, Ivkov R. Cancer therapy with iron oxide nanoparticles: agents of thermal and immune therapies. Adv Drug Deliv Rev 2020;163:65–83.
[82] Ebrahimpour A, Riahi Alam N, Abdolmaleki P, Hajipour-Verdom B, Tirgar F, Ebrahimi T, et al. Magnetic metal–organic framework based on zinc and 5-aminolevulinic acid: MR imaging and brain tumor therapy. J Inorg Organomet Polym Mater 2021;31:1208–16.
[83] Shen S, Wu L, Liu J, Xie M, Shen H, Qi X, et al. Core–shell structured Fe3O4@ TiO2-doxorubicin nanoparticles for targeted chemo-sonodynamic therapy of cancer. Int J Pharm 2015;486:380–8.
[84] Rajkumar S, Prabaharan M. Multi-functional core-shell Fe3O4@ Au nanoparticles for cancer diagnosis and therapy. Colloids Surf B Biointerfaces 2019;174:252–9.

[85] Khani T, Alamzadeh Z, Sarikhani A, Mousavi M, Mirrahimi M, Tabei M, et al. Fe3O4@ Au core–shell hybrid nanocomposite for MRI-guided magnetic targeted photo-chemotherapy. Lasers Med Sci 2022:1–9.
[86] Maleki A, Shahbazi MA, Alinezhad V, Santos HA. The progress and prospect of zeolitic imidazolate frameworks in cancer therapy, antibacterial activity, and biomineralization. Adv Healthc Mater 2020;9:2000248.
[87] Wei X, Li N, Wang Y, Xie Z, Huang H, Yang G, et al. Zeolitic imidazolate frameworks-based nanomaterials for biosensing, cancer imaging and phototheranostics. Appl Mater Today 2021;23:100995.
[88] Abdelhamid HN. Zeolitic imidazolate frameworks (ZIF-8) for biomedical applications: a review. Curr Med Chem 2021;28:7023–75.
[89] Yan J, Liu C, Wu Q, Zhou J, Xu X, Zhang L, et al. Mineralization of pH-sensitive doxorubicin prodrug in ZIF-8 to enable targeted delivery to solid tumors. Anal Chem 2020;92:11453–61.
[90] Bian R, Wang T, Zhang L, Li L, Wang C. A combination of tri-modal cancer imaging and *in vivo* drug delivery by metal–organic framework based composite nanoparticles. Biomater Sci 2015;3:1270–8.
[91] Guo P, Dutta D, Wong-Foy AG, Gidley DW, Matzger AJ. Water sensitivity in Zn4O-based MOFs is structure and history dependent. J Am Chem Soc 2015;137:2651–7.
[92] Ma A, Luo Z, Gu C, Li B, Liu J. Cytotoxicity of a metal–organic framework: drug delivery. Inorg Chem Commun 2017;77:68–71.
[93] Anarjan FS. Active targeting drug delivery nanocarriers: ligands. Nano-Struct Nano-Obj 2019;19:100370.
[94] Alijani H, Noori A, Faridi N, Bathaie SZ, Mousavi MF. Aptamer-functionalized Fe3O4@ MOF nanocarrier for targeted drug delivery and fluorescence imaging of the triple-negative MDA-MB-231 breast cancer cells. J Solid State Chem 2020;292:121680.
[95] Wu MX, Gao J, Wang F, Yang J, Song N, Jin X, et al. Multistimuli responsive core–shell nanoplatform constructed from Fe3O4@ MOF equipped with pillar [6]arene nanovalves. Small. 2018;14:1704440.
[96] Yang Y-W, Sun Y-L, Song N. Switchable host–guest systems on surfaces. Acc Chem Res 2014;47:1950–60.
[97] Li C, Wang Y, Zhang S, Zhang J, Wang F, Sun Y, et al. pH and ROS sequentially responsive podophyllotoxin prodrug micelles with surface charge-switchable and self-amplification drug release for combating multidrug resistance cancer. Drug Deliv 2021;28:680–91.
[98] Yi S, Zheng J, Lv P, Zhang D, Zheng X, Zhang Y, et al. Controlled drug release from cyclodextrin-gated mesoporous silica nanoparticles based on switchable host–guest interactions. Bioconjug Chem 2018;29:2884–91.
[99] Huang X, Wu S, Ke X, Li X, Du X. Phosphonated pillar [5] arene-valved mesoporous silica drug delivery systems. ACS Appl Mater Interfaces 2017;9:19638–45.
[100] Yang Q, Xu W, Cheng M, Zhang S, Kovaleva EG, Liang F, et al. Controlled release of drug molecules by pillararene-modified nanosystems. Chem Commun 2022;58:3255–69.
[101] Tan L-L, Li H, Qiu Y-C, Chen D-X, Wang X, Pan R-Y, et al. Stimuli-responsive metal–organic frameworks gated by pillar [5] arene supramolecular switches. Chem Sci 2015;6:1640–4.
[102] Tan L-L, Song N, Zhang SX-A, Li H, Wang B, Yang Y-W. Ca 2+, pH and thermo triple-responsive mechanized Zr-based MOFs for on-command drug release in bone diseases. J Mater Chem B 2016;4:135–40.
[103] Wang Q, Fan J, Bian X, Yao H, Yuan X, Han Y, et al. A microenvironment sensitive pillar [5] arene-based fluorescent probe for cell imaging and drug delivery. Chin Chem Lett 2022;33:1979–82.
[104] Xu J, Liu Y, Li G, Peng M, Xu S, Liu H. A reduction-triggered nanocarrier based on host–guest interaction between pillar [5] arene derivative and viologen on MSN for intracellular delivery. J Drug Deliv Sci Technol 2022;68:103055.
[105] Cheng C-A, Deng T, Lin F-C, Cai Y, Zink JI. Supramolecular nanomachines as stimuli-responsive gatekeepers on mesoporous silica nanoparticles for antibiotic and cancer drug delivery. Theranostics. 2019;9:3341.
[106] Li D, Zhang X, Chen X, Li W. Research progress and prospects for polymeric nanovesicles in anticancer drug delivery. Front Bioeng Biotechnol 2022;10:850366.
[107] Heath JL, Weiss JM, Lavau CP, Wechsler DS. Iron deprivation in cancer—potential therapeutic implications. Nutrients. 2013;5:2836–59.
[108] Zhang H, Hou L, Jiao X, Ji Y, Zhu X, Zhang Z. Transferrin-mediated fullerenes nanoparticles as Fe2+−dependent drug vehicles for synergistic anti-tumor efficacy. Biomaterials. 2015;37:353–66.
[109] Liu K, Dai L, Li C, Liu J, Wang L, Lei J. Self-assembled targeted nanoparticles based on transferrin-modified eight-arm-polyethylene glycol–dihydroartemisinin conjugate. Sci Rep 2016;6:1–12.
[110] Quijia CR, Lima C, Silva C, Alves RC, Frem R, Chorilli M. Application of MIL-100 (Fe) in drug delivery and biomedicine. J Drug Deliv Sci Technol 2021;61:102217.
[111] Wang D, Zhou J, Chen R, Shi R, Wang C, Lu J, et al. Core–shell metal-organic frameworks as Fe2+ suppliers for Fe2+−mediated cancer therapy under multimodality imaging. Chem Mater 2017;29:3477–89.
[112] Wang D, Zhou J, Chen R, Shi R, Zhao G, Xia G, et al. Controllable synthesis of dual-MOFs nanostructures for pH-responsive artemisinin delivery, magnetic resonance and optical dual-model imaging-guided chemo/photothermal combinational cancer therapy. Biomaterials. 2016;100:27–40.
[113] He J, Ramachandraiah K, Huang T, Yuan T, Liu X, Zhang H, et al. Core− shell structured hollow copper sulfide@ metal− organic framework for magnetic resonance imaging guided photothermal therapy in second near-infrared biological window. Biochem Biophys Res Commun 2023;638:51–7.
[114] Gao H, Chi B, Tian F, Xu M, Xu Z, Li L, et al. Prussian blue modified metal organic frameworks for imaging guided synergetic tumor therapy with hypoxia modulation. J Alloys Compd 2021;853:157329.
[115] Khaledian S, Nalaini F, Mehrbakhsh M, Abdoli M, Zahabi SS. Applications of novel quantum dots derived from layered materials in cancer cell imaging. FlatChem. 2021;27:100246.
[116] Tandale P, Choudhary N, Singh J, Sharma A, Shukla A, Sriram P, et al. Fluorescent quantum dots: An insight on synthesis and potential biological application as drug carrier in cancer. Biochem Biophys Reports 2021;26:100962.
[117] Nikazar S, Sivasankarapillai VS, Rahdar A, Gasmi S, Anumol P, Shanavas MS. Revisiting the cytotoxicity of quantum dots: an in-depth overview. Biophys Rev 2020;12:703–18.
[118] Yang M, Huang J, Fan J, Du J, Pu K, Peng X. Chemiluminescence for bioimaging and therapeutics: recent advances and challenges. Chem Soc Rev 2020;49:6800–15.
[119] He L, Wang T, An J, Li X, Zhang L, Li L, et al. Carbon nanodots@ zeolitic imidazolate framework-8 nanoparticles for simultaneous pH-responsive drug delivery and fluorescence imaging. CrystEngComm. 2014;16:3259–63.
[120] Perini G, Palmieri V, Ciasca G, De Spirito M, Papi M. Unravelling the potential of graphene quantum dots in biomedicine and neuroscience. Int J Mol Sci 2020;21:3712.
[121] Abánades Lázaro I, Haddad S, Rodrigo-Munoz JM, Marshall RJ, Sastre B, Del Pozo V, et al. Surface-functionalization of Zr-fumarate MOF for selective cytotoxicity and immune system compatibility in nanoscale drug delivery. ACS Appl Mater Interfaces 2018;10:31146–57.
[122] Dong S, Chen Q, Li W, Jiang Z, Ma J, Gao H. A dendritic catiomer with an MOF motif for the construction of safe and efficient gene delivery systems. J Mater Chem B 2017;5:8322–9.
[123] Singh N, Qutub S, Khashab NM. Biocompatibility and biodegradability of metal organic frameworks for biomedical applications. J Mater Chem B 2021.
[124] Wang J, Zaidi SSA, Hasnain A, Guo J, Ren X, Xia S, et al. Multitargeting peptide-functionalized star-shaped copolymers with comblike structure and a poss-core to effectively transfect endothelial cells. ACS Biomater Sci Eng 2018;4:2155–68.
[125] Baa E, Watkins GM, Krause RW, Tantoh DN. Current trend in synthesis, post-synthetic modifications and biological applications of nanometal-organic frameworks (NMOFs). Chin J Chem 2019;37:378–404.
[126] Shen D, Wang G, Liu Z, Li P, Cai K, Cheng C, et al. Epitaxial growth of γ-cyclodextrin-containing metal–organic frameworks based on a host–guest strategy. J Am Chem Soc 2018;140:11402–7.
[127] Matyjaszewski K. Advanced materials by atom transfer radical polymerization. Adv Mater 2018;30:1706441.
[128] Zoppe JO, Ataman NC, Mocny P, Wang J, Moraes J, Klok H-A. Surface-initiated controlled radical polymerization: state-of-the-art, opportunities, and challenges in surface and interface engineering with polymer brushes. Chem Rev 2017;117:1105–318.
[129] Pericleous P, Gazouli M, Lyberopoulou A, Rizos S, Nikiteas N, Efstathopoulos EP. Quantum dots hold promise for early cancer imaging and detection. Int J Cancer 2012;131:519–28.
[130] Du T, Qin Z, Zheng Y, Jiang H, Weizmann Y, Wang X. The "framework exchange"-strategy-based MOF platform for biodegradable multimodal therapy. Chem. 2019;5:2942–54.
[131] Ding J, Qu G, Chu PK, Yu XF. Black phosphorus: versatile two-dimensional materials in cancer therapies. View. 2021;2:20200043.
[132] Li Y, Liu Z, Hou Y, Yang G, Fei X, Zhao H, et al. Multifunctional nanoplatform based on black phosphorus quantum dots for bioimaging and photodynamic/photothermal synergistic cancer therapy. ACS Appl Mater Interfaces 2017;9:25098–106.
[133] Falahati M, Attar F, Sharifi M, Saboury AA, Salihi A, Aziz FM, et al. Gold nanomaterials as key suppliers in biological and chemical sensing, catalysis, and medicine. Biochim Biophys Acta (BBA)-General Subj 2020;1864:129435.
[134] Chen A, Wu L, Luo Y, Lu S, Wang Y, Zhou Z, et al. Deep tumor penetrating gold nano-adjuvant for NIR-II-triggered in situ tumor vaccination. Small. 2022;18:2200993.
[135] Huang X, El-Sayed IH, Qian W, El-Sayed MA. Cancer cell imaging and photothermal therapy in the near-infrared region by using gold nanorods. J Am Chem Soc 2006;128:2115–20.
[136] Sharifi M, Attar F, Saboury AA, Akhtari K, Hooshmand N, Hasan A, et al. Plasmonic gold nanoparticles: optical manipulation, imaging, drug delivery and therapy. J Control Release 2019;311:170–89.
[137] Sharifi M, Hosseinali SH, Alizadeh RH, Hasan A, Attar F, Salihi A, et al. Plasmonic and chiroplasmonic nanobiosensors based on gold nanoparticles. Talanta. 2020;212:120782.
[138] Wang J, Zhang HZ, Li RS, Huang CZ. Localized surface plasmon resonance of gold nanorods and assemblies in the view of biomedical analysis. TrAC Trends Anal Chem 2016;80:429–43.
[139] Choi WI, Sahu A, Kim YH, Tae G. Photothermal cancer therapy and imaging based on gold nanorods. Ann Biomed Eng 2012;40:534–46.
[140] Shen H, Liu J, Lei J, Ju H. A core–shell nanoparticle–peptide@ metal–organic framework as pH and enzyme dual-recognition switch for stepwise-responsive imaging in living cells. Chem Commun 2018;54:9155–8.
[141] An H, Li M, Gao J, Zhang Z, Ma S, Chen Y. Incorporation of biomolecules in metal-organic frameworks for advanced applications. Coord Chem Rev 2019;384:90–106.
[142] Zhong Y, Liu W, Rao C, Li B, Wang X, Liu D, et al. Recent advances in Fe-MOF compositions for biomedical applications. Curr Med Chem 2021;28:6179–98.

[143] He J, Zhang H, Zhu J, Zhang X, Liu X, Ramachandraiah K, et al. Layer-by-layer synthesis of au nanorods@ metal-organic framework core-shell nanohybrids for magnetic resonance imaging guided photothermal therapy. Mater Today Commun 2022;33:104560.
[144] Zhang L, Liu C, Gao Y, Li Z, Xing J, Ren W, et al. ZD2-engineered gold nanostar@ metal-organic framework nanoprobes for T1-weighted magnetic resonance imaging and photothermal therapy specifically toward triple-negative breast cancer. Adv Healthc Mater 2018;7:1801144.
[145] Ortiz-Castillo JE, Gallo-Villanueva RC, Madou MJ, Perez-Gonzalez VH. Anisotropic gold nanoparticles: a survey of recent synthetic methodologies. Coord Chem Rev 2020;425:213489.
[146] Dewi MR, Laufersky G, Nann T. A highly efficient ligand exchange reaction on gold nanoparticles: preserving their size, shape and colloidal stability. RSC Adv 2014;4:34217–20.
[147] Patel J, Němcová L, Maguire P, Graham W, Mariotti D. Synthesis of surfactant-free electrostatically stabilized gold nanoparticles by plasma-induced liquid chemistry. Nanotechnology. 2013;24:245604.
[148] Chien W-C, Cheng P-H, Cheng X-J, Chuang C-C, Huang Y-T, TS A, et al.. MCP-1-functionalized, core–shell gold nanorod@ iron-based metal–organic framework (MCP-1/GNR@ MIL-100 (Fe)) for photothermal therapy. ACS Appl Mater Interfaces 2021;13(44):52092–105.
[149] Lin ZP, Nguyen LN, Ouyang B, MacMillan P, Ngai J, Kingston BR, et al. Macrophages actively transport nanoparticles in tumors after extravasation. ACS Nano 2022;16:6080–92.
[150] Khatoon N, Zhang Z, Zhou C, Chu M. Macrophage membrane coated nanoparticles: a biomimetic approach for enhanced and targeted delivery. Biomater Sci 2022;10(5):1193–208.
[151] Xu W-J, Cai J-X, Li Y-J, Wu J-Y, Xiang D. Recent progress of macrophage vesicle-based drug delivery systems. Drug Deliv Transl Res 2022:1–16.
[152] Richards DM, Hettinger J, Feuerer M. Monocytes and macrophages in cancer: development and functions. Cancer Microenviron 2013;6:179–91.
[153] Chen X-J, Deng Y-R, Wang Z-C, Wei W-F, Zhou C-F, Zhang Y-M, et al. Hypoxia-induced ZEB1 promotes cervical cancer progression via CCL8-dependent tumour-associated macrophage recruitment. Cell Death Dis 2019;10:1–11.
[154] Kang SU, Cho SY, Jeong H, Han J, Chae HY, Yang H, et al. Matrix metalloproteinase 11 (MMP11) in macrophages promotes the migration of HER2-positive breast cancer cells and monocyte recruitment through CCL2–CCR2 signaling. Lab Invest 2022;102:376–90.
[155] Tu W, Gong J, Zhou Z, Tian D, Wang Z. TCF4 enhances hepatic metastasis of colorectal cancer by regulating tumor-associated macrophage via CCL2/CCR2 signaling. Cell Death Dis 2021;12:1–15.
[156] Zhang F, Li P, Liu S, Yang M, Zeng S, Deng J, et al. β-Catenin-CCL2 feedback loop mediates crosstalk between cancer cells and macrophages that regulates breast cancer stem cells. Oncogene. 2021;40:5854–65.
[157] Zhang T, Qin L, Liu L, Zhang M, Du T, Fan Y, et al. A smart nanoprobe based on luminescent terbium metal–organic framework coated gold nanorods for monitoring and photo-stimulated combined thermal-chemotherapy. J Rare Earths 2022 Sep 1;40(9):1371–81.
[158] Guo H, Yi S, Feng K, Xia Y, Qu X, Wan F, et al. In situ formation of metal organic framework onto gold nanorods/mesoporous silica with functional integration for targeted theranostics. Chem Eng J 2021;403:126432.
[159] Li R-T, Zhu Y-D, Li W-Y, Hou Y-K, Zou Y-M, Zhao Y-H, et al. Synergistic photothermal-photodynamic-chemotherapy toward breast cancer based on a liposome-coated core–shell AuNS@ NMOFs nanocomposite encapsulated with gambogic acid. J Nanobiotechnol 2022;20:1–22.
[160] Neufeld MJ, Winter H, Landry MR, Goforth AM, Khan S, Pratx G, et al. Lanthanide metal–organic frameworks for multispectral radioluminescent imaging. ACS Appl Mater Interfaces 2020;12:26943–54.
[161] Cheng H, Sun Q, Wang S, Zhang Y, Fan D, Huang JJ, et al. Elucidating energy-transfer dynamics within and beyond lanthanide metal–organic frameworks. J Phys Chem C 2019;123:30165–70.
[162] Weishäupl S, Mayer D, Cui Y, Kumar P, Oberhofer H, Fischer RA, et al. Recent advances of multiphoton absorption in metal-organic frameworks. J Mater Chem C 2022;10(18):6912–34.
[163] Du C, Wu X, He M, Zhang Y, Zhang R, Dong C-M. Polymeric photothermal agents for cancer therapy: recent progress and clinical potential. J Mater Chem B 2021;9:1478–90.
[164] Li Y, Jin J, Wang D, Lv J, Hou K, Liu Y, et al. Coordination-responsive drug release inside gold nanorod@ metal-organic framework core–shell nanostructures for near-infrared-induced synergistic chemo-photothermal therapy. Nano Res 2018;11:3294–305.
[165] Gao G, Jiang YW, Guo Y, Jia HR, Cheng X, Deng Y, et al. Enzyme-mediated tumor starvation and phototherapy enhance mild-temperature photothermal therapy. Adv Funct Mater 2020;30:1909391.
[166] Gao S, Yang D, Fang Y, Lin X, Jin X, Wang Q, et al. Engineering nanoparticles for targeted remodeling of the tumor microenvironment to improve cancer immunotherapy. Theranostics. 2019;9:126.
[167] Kraehenbuehl L, Weng C-H, Eghbali S, Wolchok JD, Merghoub T. Enhancing immunotherapy in cancer by targeting emerging immunomodulatory pathways. Nat Rev Clin Oncol 2022;19:37–50.
[168] Green DR. The coming decade of cell death research: five riddles. Cell. 2019;177:1094–107.
[169] Liu J, Miao L, Sui J, Hao Y, Huang G. Nanoparticle cancer vaccines: design considerations and recent advances. Asian J Pharm Sci 2020;15:576–90.
[170] Birge R, Boeltz S, Kumar S, Carlson J, Wanderley J, Calianese D, et al. Phosphatidylserine is a global immunosuppressive signal in efferocytosis, infectious disease, and cancer. Cell Death Differ 2016;23:962–78.
[171] Chang W, Fa H, Xiao D, Wang J. Targeting phosphatidylserine for cancer therapy: prospects and challenges. Theranostics. 2020;10:9214.
[172] Li L, Zou J, Dai Y, Fan W, Niu G, Yang Z, et al. Burst release of encapsulated annexin A5 in tumours boosts cytotoxic T-cell responses by blocking the phagocytosis of apoptotic cells. Nat Biomed Eng 2020;4:1102–16.
[173] Bricogne C, Fine M, Pereira PM, Sung J, Tijani M, Wang Y, et al. TMEM16F activation by Ca2+ triggers plasma membrane expansion and directs PD-1 trafficking. Sci Rep 2019;9:1–13.
[174] Dai Z, Wang Q, Tang J, Wu M, Li H, Yang Y, et al. Immune-regulating bimetallic metal-organic framework nanoparticles designed for cancer immunotherapy. Biomaterials. 2022;280:121261.
[175] Banerjee R, Furukawa H, Britt D, Knobler C, O'Keeffe M, Yaghi OM. Control of pore size and functionality in isoreticular zeolitic imidazolate frameworks and their carbon dioxide selective capture properties. J Am Chem Soc 2009;131:3875–7.
[176] Manzano M, Vallet-Regí M. Mesoporous silica nanoparticles for drug delivery. Adv Funct Mater 2020;30:1902634.
[177] Zheng C, Wang Y, Phua SZF, Lim WQ, Zhao Y. ZnO–DOX@ ZIF-8 core–shell nanoparticles for pH-responsive drug delivery. ACS Biomater Sci Eng 2017;3:2223–9.
[178] Xiao X, Liang S, Zhao Y, Huang D, Xing B, Cheng Z, et al. Core–shell structured 5-FU@ ZIF-90@ ZnO as a biodegradable nanoplatform for synergistic cancer therapy. Nanoscale. 2020;12:3846–54.
[179] Liu Y, Gong CS, Lin L, Zhou Z, Liu Y, Yang Z, et al. Core-shell metal-organic frameworks with fluorescence switch to trigger an enhanced photodynamic therapy. Theranostics. 2019;9:2791.
[180] Gao Z, Li Y, Zhang Y, Cheng K, An P, Chen F, et al. Biomimetic platinum nanozyme immobilized on 2D metal–organic frameworks for mitochondrion-targeting and oxygen self-supply photodynamic therapy. ACS Appl Mater Interfaces 2019;12:1963–72.
[181] Zhang W, Li S, Liu X, Yang C, Hu N, Dou L, et al. Oxygen-generating MnO2 nanodots-anchored versatile nanoplatform for combined chemo-photodynamic therapy in hypoxic cancer. Adv Funct Mater 2018;28:1706375.
[182] He Z, Huang X, Wang C, Li X, Liu Y, Zhou Z, et al. A catalase-like metal-organic framework nanohybrid for O2-evolving synergistic chemoradiotherapy. Angew Chem 2019;131:8844–8.
[183] Liu C, Luo L, Zeng L, Xing J, Xia Y, Sun S, et al. Porous gold nanoshells on functional NH2-MOFs: facile synthesis and designable platforms for cancer multiple therapy. Small. 2018;14:1801851.
[184] Qin N, Wu X, Liu X, Xue Z-H, Muddassir M, Sakiyama H, et al. Well-arranged hollow Au@Zn/Ni-MOF-2-NH2 core–shell nanocatalyst with enhanced catalytic activity for biomass-derived d-xylose oxidation. ACS Sustain Chem Eng 2022;10:5396–403.
[185] Qin N, Pan A, Yuan J, Ke F, Wu X, Zhu J, et al. One-step construction of a hollow au@bimetal–organic framework core–shell catalytic nanoreactor for selective alcohol oxidation reaction. ACS Appl Mater Interfaces 2021;13:12463–71.
[186] Liu Z, Li T, Han F, Wang Y, Gan Y, Shi J, et al. A cascade-reaction enabled synergistic cancer starvation/ROS-mediated/chemo-therapy with an enzyme modified Fe-based MOF. Biomater Sci 2019;7:3683–92.
[187] Ding S-S, He L, Bian X-w, Tian G. Metal-organic frameworks-based nanozymes for combined cancer therapy. Nano Today 2020;35:100920.
[188] Falahati M, Sharifi M, Ten Hagen TL. Explaining chemical clues of metal organic framework-nanozyme nano−/micro-motors in targeted treatment of cancers: benchmarks and challenges. J Nanobiotechnol 2022;20:1–26.
[189] Zhou N, Su F, Guo C, He L, Jia Z, Wang M, et al. Two-dimensional oriented growth of Zn-MOF-on-Zr-MOF architecture: a highly sensitive and selective platform for detecting cancer markers. Biosens Bioelectron 2019;123:51–8.
[190] Wang D, Zhao C, Gao G, Xu L, Wang G, Zhu P. Multifunctional NaLnF4@ MOF-Ln nanocomposites with dual-mode luminescence for drug delivery and cell imaging. Nanomaterials. 2019;9:1274.
[191] Jia M, Yang X, Chen Y, He M, Zhou W, Lin J, et al. Grafting of Gd-DTPA onto MOF-808 to enhance MRI performance for guiding photothermal therapy. J Mater Chem B 2021;9:8631–8.
[192] Xiang X, Pang H, Ma T, Du F, Li L, Huang J, et al. Ultrasound targeted microbubble destruction combined with Fe-MOF based bio−/enzyme-mimics nanoparticles for treating of cancer. J Nanobiotechnol 2021;19:1–14.
[193] Yang B, Ding L, Yao H, Chen Y, Shi J. A metal-organic framework (MOF) fenton nanoagent-enabled nanocatalytic cancer therapy in synergy with autophagy inhibition. Adv Mater 2020;32:1907152.
[194] Sun X, He G, Xiong C, Wang C, Lian X, Hu L, et al. One-pot fabrication of hollow porphyrinic MOF nanoparticles with ultrahigh drug loading toward controlled delivery and synergistic cancer therapy. ACS Appl Mater Interfaces 2021;13:3679–93.
[195] Ventura K, Arrieta RA, Marcos-Hernández M, Jabbari V, Powell CD, Turley R, et al. Superparamagnetic MOF@ GO Ni and Co based hybrid nanocomposites as efficient water pollutant adsorbents. Sci Total Environ 2020;738:139213.
[196] Pooresmaeil M, Asl EA, Namazi H. A new pH-sensitive CS/Zn-MOF@ GO ternary hybrid compound as a biofriendly and implantable platform for prolonged 5-fluorouracil delivery to human breast cancer cells. J Alloys Compd 2021;885:160992.
[197] Mokri N, Sepehri Z, Faninam F, Khaleghi S, Kazemi NM, Hashemi M. Chitosan-coated Zn-metal-organic framework nanocomposites for effective targeted

delivery of LNA-antisense miR-224 to colon tumor: *in vitro* studies. Gene Ther 2021:1–11.
[198] Cao X-X, Liu S-L, Lu J-S, Zhang Z-W, Wang G, Chen Q, et al. Chitosan coated biocompatible zeolitic imidazolate framework ZIF-90 for targeted delivery of anticancer drug methotrexate. J Solid State Chem 2021;300:122259.
[199] Esmaeili Y, Khavani M, Bigham A, Sanati A, Bidram E, Shariati L, et al. Mesoporous silica@ chitosan@ gold nanoparticles as "on/off" optical biosensor and pH-sensitive theranostic platform against cancer. Int J Biol Macromol 2022; 202:241–55.
[200] Ijaz H, Tulain UR, Minhas MU, Mahmood A, Sarfraz RM, Erum A, et al. Design and *in vitro* evaluation of pH-sensitive crosslinked chitosan-grafted acrylic acid copolymer (CS-co-AA) for targeted drug delivery. Int J Polym Mater Polym Biomater 2022;71:336–48.
[201] Li S, Zhang H, Chen K, Jin M, Vu SH, Jung S, et al. Application of chitosan/alginate nanoparticle in oral drug delivery systems: prospects and challenges. Drug Deliv 2022;29:1142–9.
[202] Lin C, Sun K, Zhang C, Tan T, Xu M, Liu Y, et al. Carbon dots embedded metal organic framework@ chitosan core-shell nanoparticles for vitro dual mode imaging and pH-responsive drug delivery. Microporous Mesoporous Mater 2020; 293:109775.
[203] Giliopoulos D, Zamboulis A, Giannakoudakis D, Bikiaris D, Triantafyllidis K. Polymer/metal organic framework (MOF) nanocomposites for biomedical applications. Molecules. 2020;25:185.
[204] Pan J, Li Y, Chen K, Zhang Y, Zhang H. Enhanced physical and antimicrobial properties of alginate/chitosan composite aerogels based on electrostatic interactions and noncovalent crosslinking. Carbohydr Polym 2021;266:118102.
[205] Hu L, Xiong C, Wei G, Yu Y, Li S, Xiong X, et al. Stimuli-responsive charge-reversal MOF@ polymer hybrid nanocomposites for enhanced co-delivery of chemotherapeutics towards combination therapy of multidrug-resistant cancer. J Colloid Interface Sci 2022;608:1882–93.
[206] Wu B, Fu J, Zhou Y, Luo S, Zhao Y, Quan G, et al. Tailored core–shell dual metal–organic frameworks as a versatile nanomotor for effective synergistic antitumor therapy. Acta Pharm Sin B 2020;10:2198–211.
[207] Trushina DB, Sapach AY, Burachevskaia OA, Medvedev PV, Khmelenin DN, Borodina TN, et al. Doxorubicin-loaded core–shell UiO-66@ SiO2 metal–organic frameworks for targeted cellular uptake and cancer treatment. Pharmaceutics. 2022;14:1325.
[208] Wang LJ, Deng H, Furukawa H, Gándara F, Cordova KE, Peri D, et al. Synthesis and characterization of metal–organic framework-74 containing 2, 4, 6, 8, and 10 different metals. Inorg Chem 2014;53:5881–3.
[209] Lu W, Wei Z, Gu Z-Y, Liu T-F, Park J, Park J, et al. Tuning the structure and function of metal–organic frameworks via linker design. Chem Soc Rev 2014;43: 5561–93.
[210] Kitagawa S. Metal–organic frameworks (MOFs). Chem Soc Rev 2014;43:5415–8.
[211] Ebrahimi AK, Barani M, Sheikhshoaie I. Fabrication of a new superparamagnetic metal-organic framework with core-shell nanocomposite structures: characterization, biocompatibility, and drug release study. Mater Sci Eng C 2018; 92:349–55.
[212] Chen R, Zhang J, Wang Y, Chen X, Zapien JA, Lee C-S. Graphitic carbon nitride nanosheet@ metal–organic framework core–shell nanoparticles for photo-chemo combination therapy. Nanoscale. 2015;7:17299–305.
[213] Shang W, Zeng C, Du Y, Hui H, Liang X, Chi C, et al. Core–shell gold nanorod@ metal–organic framework nanoprobes for multimodality diagnosis of glioma. Adv Mater 2017;29:1604381.
[214] Ren S-Z, Wang B, Zhu X-H, Zhu D, Liu M, Li S-K, et al. Oxygen self-sufficient core–shell metal–organic framework-based smart nanoplatform for enhanced synergistic chemotherapy and photodynamic therapy. ACS Appl Mater Interfaces 2020;12:24662–74.
[215] Wang F, Zhang Y, Liu Z, Du Z, Zhang L, Ren J, et al. A biocompatible heterogeneous MOF–Cu catalyst for in vivo drug synthesis in targeted subcellular organelles. Angew Chem Int 2019;58(21):6987–92.
[216] Sun T, Zhang YS, Pang B, Hyun DC, Yang M, Xia Y. Engineered nanoparticles for drug delivery in cancer therapy. Nanomater Neoplasms 2021:31–142.
[217] Yin SY, Song G, Yang Y, Zhao Y, Wang P, Zhu LM, et al. Persistent regulation of tumor microenvironment via circulating catalysis of MnFe2O4@ metal–organic frameworks for enhanced photodynamic therapy. Adv Funct Mater 2019;29: 1901417.
[218] Yu B, Wang Y-J, Lin Y-Y, Feng Y, Wu J, Liu W-S, et al. HKUST-1 nano metal–organic frameworks combined with ZnGa 2 O 4: Cr 3+ near-infrared persistent luminescence nanoparticles for *in vivo* imaging and tumor chemodynamic and photothermal synergic therapy. Nanoscale. 2022;14: 8978–85.
[219] Zeng JY, Zhang MK, Peng MY, Gong D, Zhang XZ. Porphyrinic metal–organic frameworks coated gold nanorods as a versatile nanoplatform for combined photodynamic/photothermal/chemotherapy of tumor. Adv Funct Mater 2018;28: 1705451.
[220] Zhou G, Li M. Near-infrared-II plasmonic trienzyme-integrated metal–organic frameworks with high-efficiency enzyme cascades for synergistic trimodal oncotherapy. Adv Mater 2022;2200871.
[221] Nie Z, Vahdani Y, Cho WC, Bloukh SH, Edis Z, Haghighat S, et al. 5-fluorouracil-containing inorganic iron oxide/platinum nanozymes with dual drug delivery and enzyme-like activity for the treatment of breast cancer. Arab J Chem 2022;15: 103966.
[222] Liu X, Zhu X, Qi X, Meng X, Xu K. Co-administration of iRGD with Sorafenib-loaded iron-based metal-organic framework as a targeted ferroptosis agent for liver cancer therapy. Int J Nanomedicine 2021;16:1037.